TECHNOLOGY DEVELOPMENT FOR IRON FISCHER-TROPSCH CATALYSIS

Contract No. DE-AC22-94PC94055

Final Report

Prepared for

U.S. Department of Energy
Federal Energy Technology Center
FETC Project Manager: Richard E. Tischer
P. O. Box 10940
Pittsburgh, PA 15236-0940

Submitted By

Project Manager: Burtron H. Davis
University of Kentucky Research Foundation
Kinkead Hall
Lexington, KY 40506-0057

Submitted
December 15, 1998

Disclaimer

"This report was prepared as an account of work sponsored by an agency of the United States Government. Neither the United States Government nor any agency thereof, nor any of their employees, makes any warranty, express or implied, or assumes any legal liability or responsibility for the accuracy, completeness, or usefulness of any information, apparatus, product, or process disclosed, or represents that its use would not infringe privately owned rights. Reference herein to any specific commercial product, process, or service by trade name, trademark, manufacturer, or otherwise does not necessarily constitute or imply its endorsement, recommendation or favoring by the United States Government or any agency thereof. The views and opinions of authors expressed herein do not necessarily state or reflect those of the United States Government or any agency thereof."

Abstract

The goal of the proposed work is the development of iron-based Fischer-Tropsch catalysts that combined high activity, selectivity and life with physical robustness for slurry phase reactors that will produce either low-alpha or high-alpha products. The catalyst that is developed will be suitable for testing at the Advanced Fuels Development Facility at LaPorte, Texas or similar sized plant. Previous work by the offeror has produced a catalyst formulation that is 1.5 times as active as the "standard-catalyst" developed by German workers for slurry phase synthesis. The proposed work will optimize the catalyst composition and pretreatment operation for this low-alpha catalyst. In parallel, work will be conducted to design a high-alpha iron catalyst that is suitable for slurry phase synthesis. Studies will be conducted to define the chemical phases present at various stages of the pretreatment and synthesis stages and to define the course of these changes. The oxidation/reduction cycles that are anticipated to occur in large, commercial reactors will be studied at the laboratory scale. Catalyst performance will be determined for catalysts synthesized in this program for activity, selectivity and aging characteristics.

Table of Contents

1.0.0 Executive Summary

The work with low-alpha iron catalysts has defined formulations that have activity equal to or superior to current catalysts. For these catalysts, it has been demonstrated that the hydrocarbon productivity per unit of iron catalyst dramatically depends upon CO conversion. For CO conversions in the 30-50% range, hydrocarbon productivity exceeds 2 g h.c./g Fe-hr, a very high productivity rate. These iron catalysts are stable, with declines in CO conversions being less than 1% CO/week during five months of testing. Process schemes have been advanced to take advantage of these catalysts.

In the 30-50% CO conversion range, the fraction of CO converted to hydrocarbons with the low-alpha catalyst was in the 60-70% range. In other words, the conversion ratio for H_2/CO is in the range of 1.5-1.6; this approaches the usage ratio expected for cobalt catalysts.

Iron catalysts with adequate activity for high-alpha (heavy wax) synthesis have been prepared. These catalysts have low methane selectivity. However, the internal filters have become plugged with catalyst fines/wax so that runs exceeding 500 hours cannot be made. Wax/slurry problems must be solved if long-term testing is to be accomplished. In contrast to the iron catalysts, operation for 750 hours have been accomplished in the same reactor set-up with supported cobalt catalysts.

Low temperature (230^{o}C), slurry phase Fischer-Tropsch synthesis (FTS) was conducted with precipitated iron-silicon catalysts under industrially relevant conditions (flow=3.1 NL h^{-1}g-Fe^{-1}, H_2:CO=0.7, P=1.31 MPa). The effects of activation gas (hydrogen, carbon monoxide or syngas) and promoters (potassium and copper) on activity and selectivity were explored. Optimum potassium promotion was in the range

of 4-5 atomic percent, relative to iron for these high-alpha, low-temperature catalysts. Promotion with copper lowered the reduction temperature and increased FTS activity, regardless of the activation gas used. Carbon monoxide activation gave the highest activity for a 100Fe/4.4Si/5.2K catalyst (atomic percent, relative to iron) while syngas activation was superior for a 100Fe/4.4Si/2.6Cu/5.2K catalyst. Selectivity of the FTS product was not affected by the activation gas employed or copper promotion; however, potassium promotion increased wax and alkene selectivity. A syngas activated 100Fe/4.4Si/2.6Cu/5.2K catalyst gave the best overall performance at 230^{o}C. Alkene selectivity was greater than 75% for the C_2-C_{11} fraction, methane selectivity was below 3 wt% and C_{12}+ selectivity was above 70 wt%.

The effect of potassium on catalyst activity, kinetic parameters and selectivity has been investigated for a precipitated iron catalyst that was employed with low H_2/CO ratio typical of a synthesis gas generated from coal. A wide range of synthesis gas conversions have been obtained by varying space velocities over catalysts with various potassium loadings. Differing trends in catalyst activity with potassium loading were observed depending on the space velocity or synthesis gas conversion. As potassium loading increased, the catalyst activity either decreased (low conversions), passed through a maximum (intermediate conversions) or increased (high conversions). This is shown to be a result of the increasing dependency of the Fischer-Tropsch synthesis on the hydrogen formed by the water-gas shift reaction with increasing synthesis gas conversions. Both the rate constant and the adsorption parameter in a common two-parameter Fischer-Tropsch rate expression decreased with potassium loading; therefore, observed maxima in Fischer-Tropsch rate with potassium loading can be due to the opposing influences of these parameters. The effect of potassium on alkene

selectivity was dependent on the number of carbon atoms of the hydrocarbons as well as the carbon monoxide conversion level. The extent of isomerization of alkene products decreased with potassium loading, while the selectivity to methane decreased with increasing potassium content at CO conversions about 50% and higher.

A consistent explanation for these activity trends has been given. The overall FTS activity is independent of the WGS reaction at low synthesis gas conversions. Potassium acts as a catalyst poison at these conversion levels as the FTS activity decreases with potassium loading. As the synthesis gas conversion increases, the hydrogen supplied to the reactor is insufficient for the FTS and the FTS increasingly depends on the hydrogen formed by the WGS reaction. Further, the extent of the WGS reaction increases with potassium loading. Thus as synthesis gas conversion increases the maximum overall FTS activity is obtained first at intermediate potassium loadings and finally at the highest potassium loading used in this study.

Unlike previous studies, the effect of potassium on catalyst selectivity has been compared at similar conversions. The effect of increasing amounts of potassium on alkene selectivity depends on the number of carbon atoms of the hydrocarbons as well as the carbon monoxide conversion level. The extent of isomerization decreases with potassium loading. The selectivity to methane in the total hydrocarbon product is affected by potassium at carbon monoxide conversions above 50% and increases with decreasing potassium loading.

The equilibrium phase compositions of iron have been calculated for gas compositions that could be encountered during the Fischer-Tropsch synthesis. The gas compositions measured experimentally for CO conversion levels in the 30-90% range show that iron should be present as the carbide phase. However, experimental

characterization of iron catalysts show that a significant fraction of the iron is present as Fe_3O_4 following synthesis for several days. A model that can account for the experimental catalyst phase composition and the gases present in the reactor would have a core of Fe_3O_4 and an outer layer of iron carbides.

Slurry phase Fischer-Tropsch Synthesis (FTS) was conducted with two precipitated iron catalysts (100Fe/3.6Si/0.71K and 100Fe/4.4Si/1.0K, atomic % relative to Fe) at 543K, 1.31MPa and a synthesis gas (H_2/CO=0.7) space velocity of 3.1 NL h^{-1} g Fe^{-1}. The impact of activation gas (CO, H_2/CO=0.7 or H_2/CO=0.1), temperature (543K or 573K) and pressure (1.31MPa or 0.10 MPa) on the long term (>500 h) activity and selectivity of the catalysts were explored. Pretreatment with CO under the conditions employed gave highly active and stable catalysts. Catalyst performance when synthesis gas activation was used was found to be dependent upon the partial pressure of hydrogen in the activating gas with low hydrogen partial pressures resulting in the highest catalyst activity. X-ray diffraction results indicate that carbon monoxide activations and synthesis gas activations with low hydrogen partial pressure result in the formation of the carbides ?-Fe_5C_2 and e-$Fe_{2.2}C$ while activation with synthesis gas with high hydrogen partial pressure results in the formation of only Fe_3O_4. It was found that treating the 100/3.6Si/0.71K catalyst activated with synthesis gas at 1.31 MPa and 543K, with carbon monoxide caused the activity to increase dramatically and the Fe_3O_4 to be partially converted to iron carbides. It is concluded that Fe_3O_4 is relatively inactive for FTS while the presence of some bulk iron carbide is necessary for high FTS activity to be achieved.

CO pretreatment of precipitated Fe/Si/K catalysts consistently results in high FTS activity because active carbide phases are readily formed. In the case of syngas

activation, there is a relationship between the hydrogen partial pressure in the activation gas and the initial FTS activity. During activation with syngas, the catalyst is exposed to carbon dioxide and water as well as carbon monoxide and hydrogen. It has been found that during activations with high partial pressures of hydrogen, enough water is formed to prevent the catalyst from being reduced to active iron carbide phases and only relatively inactive Fe_3O_4 is formed. The results of this study indicate that the formation of an iron carbide (?-Fe_5C_2 and/or e\-$Fe_{2.2}C$) is necessary for high FTS activity; however, based on previous Mössbauer spectroscopy experiments, the activity of iron catalysts is not related to the amount of bulk iron carbide present [3]. These results indicate that a layer of surface carbide may be responsible for FTS activity.

Iron catalysts undergo conversion from Fe_2O_3 to iron carbides during activation and a significant fraction of the carbide is converted back to Fe_3O_4 during use. Based upon X-ray densities of the compounds, contraction and/or expansion of the particle values may approach 100%, potentially creating severe strains that could cause particle disintegration. To overcome this problem, supported iron catalysts may be employed. Preliminary studies indicate the silica and alumina supports have sufficient robustness to survive testing in the CSTR without significant size reduction.

Physical measurements are currently unavailable that permit a prediction of catalyst robustness. Several typical catalyst and/or support materials and Fe_2O_3 catalyst particles were used for microhardness testing. The iron oxide sample was so soft that the standard hardness tests cannot be used to make reliable measurements, indicating that iron oxide is extremely soft.

Extensive use of electron microscopy and Mössbauer spectroscopy was made using a variety of iron catalysts collected at various times during activation and use. However, while the results are of interest, the characterization data do not relate directly to catalyst performance.

Deactivation rates and aged catalyst properties have been investigated as a function of time on stream for iron-based Fischer-Tropsch catalysts in the presence/absence of potassium and/or silicon. There is a synergism in activity maintenance with the addition of both potassium and silicon to an iron catalyst. The addition of silicon appears to stabilize the surface area of the catalyst. Catalysts containing only iron or added silicon with or without potassium consist mainly of iron oxide at the end of the run. However, iron carbides are the dominant phase of the iron catalyst with added potassium alone. Catalyst surface areas increase slightly during synthesis. The bulk phase of the catalyst does not correlate to the catalyst activity. The partial pressure of water in the reactor is lower for potassium-containing catalysts and is not a reliable predictor of catalyst deactivation rate.

Fischer-Tropsch synthesis (FTS) was studied using a precipitated Fe/K catalyst in a improved short slurry bubble column reactor (SBCR) equipped with a satisfactory reactor-wax separation system and a continuous stirred tank reactor (CSTR) using the same experiment conditions. The catalyst in the SBCR had a lower catalytic activity. Methane and the products of the gas are higher in the CSTR. Some effects may be related to different mixing heat, mass transfer phenomena between two reactors. The C_3+ hydrocarbons (C_3+H.C.) with synthesis gas ($CO+H_2$) conversion ratio had similar values.

The solvent used for start-up may have impact upon the subsequent performance of the catalyst. Our study using a light (average molecular weight 420) and a heavy (average molecular weight 3000) start-up solvent produced the same results, indicating that the viscosity and/or molecular weight do not impact the catalyst performance (activity and aging).

In comparing silica and alumina as structural promoters, it has been found that silica is superior to alumina. A catalyst containing an intermediate amount of alumina appears to provide the superior catalyst.

During these studies five different modifications have been made to the CSTR in order to remove wax when operating with precipitated, high-alpha iron catalysts. Improvements have been made; however, with 10% slurry and higher concentrations we have not been able to operate for longer than about 400-500 hours. This factor continues to be a major problem to overcome in our study of high-alpha, precipitated iron catalysts.

A technical assessment comparing published results with iron and cobalt catalysts for use with low H_2/CO ratios (coal-derived) and high H_2/CO ratios (natural gas derived) synthesis gas has been completed and is included at the end of this report.

Significant improvements in the analysis of Fischer-Tropsch products (to carbon number 90) have been made. This includes writing programs to transfer data directly to a computer and to automatically utilize this data to generate graphics.

2.0.0 Introduction

The objective of this research project is to develop the technology for the production of physically robust iron-based Fischer-Tropsch catalysts that have suitable

activity, selectivity and stability to be used in the slurry phase synthesis reactor development. The catalysts that are developed shall be suitable for testing in the Advanced Fuels Development Facility at LaPorte, Texas, to produce either low- or high-alpha product distributions. Previous work by the offeror has produced a catalyst formulation that is 1.5 times as active as the "standard-catalyst" developed by German workers for slurry phase synthesis. The proposed work will optimize the catalyst composition and pretreatment operation for this low-alpha catalyst. In parallel, work will be conducted to design a high-alpha iron catalyst this is suitable for slurry phase synthesis. Studies will be conducted to define the chemical phases present at various stages of the pretreatment and synthesis stages and to define the course of these changes. The oxidation/reduction cycles that are anticipated to occur in large, commercial reactors will be studied at the laboratory scale. Catalyst performance will be determined for catalysts synthesized in this program for activity, selectivity and aging characteristics.

The research is divided into four major topical areas: (a) catalyst preparation and characterization, (b) product characterization, (c) reactor operations, and (d) data assessment.

To accomplish the objectives of the project, these topics have been organized into the following technical tasks:

a. Task 1.0 Development of Optimum Promoter Levels for Low- and High-Alpha Catalysts

The goal of this task is to identify and optimize procedure for the preparation of iron-based catalysts that combine high activity selectivity and life with physical robustness. Each of the subtasks address an area of considerable uncertainty in the synthesis of catalysts.

1.1 Determine Optimized Synthesis Procedure for High-Alpha Iron-Based Fischer-Tropsch Catalysts

- Role of precursor particle size on activity.
- Role of Cu in precipitated catalysts.
- Define attrition resistance.

1.2 Prepare Catalysts that can be Used to Determine the Role of Promoters for Low- and High-Alpha Catalysts

- Define optimum SiO_2.
- Define optimum Al_2O_3.

1.3 Prepare Catalysts that can be Used to Quantify the Role of K on Product Selectivity in both Low- and High-Alpha Catalysts.

1.4 Complete the Optimization of the Two Best Low-Alpha, Iron-Based Fischer-Tropsch Catalysts Developed during the Previous Contract.

b. Task 2.0 Definition of Preferred Pretreatment for both Low- and High-Alpha Fischer-Tropsch Catalysts.

The goals of this task are to define the preferred treatment, to define the role of Cu and K during the pretreatment on activity and selectivity and to define the chemical

and physical changes which occur during the preferred pretreatment. The subtasks address each of these goals.

2.1 Determine the Role of Cu in the Activation of Precipitated Low- and High-Alpha, Iron-Based Fischer-Tropsch Catalysts.

2.2 Determine the Effect of K Content on Activation Procedures and Determine if the Method of Addition has any Effect on Catalyst Activity and Life.

2.3 Determine the Physical and Chemical Changes that Occur during Catalyst Pretreatment and Use and Determine how these Changes Effect the Strength of the Catalysts.

2.4 Evaluate the Effect of Carbon Deposition during Catalyst Activation on Activity, Selectivity and Aging Characteristics.

c. Task 3.0 Catalyst Structure and Characterization.

The goal of this task is to provide basic analyses (surface area, XRD) of all catalyst prepared and to provide additional techniques as required (Mössbauer, SEM, XPS, etc.) to answer specific questions or to provide basic required characterization data for the catalysts.

d. Task 4.0 Catalyst Testing.

The goals of this task are to operate the eight CSTR reactors, measure catalyst performance, determine the stable phases that exist during synthesis at low and high conversions and to determine the rates of interconversion of iron oxide and carbide.

4.1 Verify the Quality of Data Obtained from the CSTR's.

4.2 Measure Catalyst Performance.

4.3 Determine the Stable Phases that Exist during Synthesis at Low and High CO Conversion Levels.

4.4 Obtain Data on the Rates Involved in the Interconversion of Iron Oxide and Iron Carbide.

3.0.0 Results and Discussion

3.1.0 Task 1. Development of the Optimum Promoter Levels for Low- and High-Alpha Iron Based Fischer-Tropsch Catalysts and Task 2. The Definition of the Preferred Pretreatment of Low- and High-Alpha Catalysts

3.1.1 Activity and Selectivity of Precipitated Iron Fischer-Tropsch Catalysts

ABSTRACT

Low temperature (230^{o}C), slurry phase Fischer-Tropsch synthesis (FTS) was conducted with precipitated iron-silicon catalysts under industrially relevant conditions (flow=3.1 NL $h^{-1}g\text{-}Fe^{-1}$, H_2:CO=0.7, P=1.31 MPa). The effects of activation gas (hydrogen, carbon monoxide or syngas) and promoters (potassium and copper) on activity and selectivity were explored. Optimum potassium promotion was in the range of 4-5 atomic percent, relative to iron for these high-alpha, low-temperature catalysts. Promotion with copper lowered the reduction temperature and increased FTS activity, regardless of the activation gas used. Carbon monoxide activation gave the highest activity for a 100Fe/4.4Si/5.2K catalyst (atomic percent, relative to iron) while syngas activation was superior for a 100Fe/4.4Si/2.6Cu/5.2K catalyst. Selectivity of the FTS product was not affected by the activation gas employed or copper promotion; however, potassium promotion increased wax and alkene selectivity. A syngas activated 100Fe/4.4Si/2.6Cu/5.2K catalyst gave the best overall performance at 230^{o}C. Alkene

selectivity was greater than 75% for the C_2-C_{11} fraction, methane selectivity was below 3 wt% and C_{12}+ selectivity was above 70 wt%.

INTRODUCTION

The Fischer-Tropsch synthesis (FTS) offers the potential of converting syngas into high value chemicals [1-3]. Although several metals are active for the FTS, only iron and cobalt catalysts appear economically feasible on an industrial scale [4]. The high water-gas shift activity of iron makes it an ideal catalyst for converting hydrogen lean syngas derived from coal [4,5]. Controlling selectivity is an important aspect of FTS catalyst development. Cobalt catalysts have a high activity for hydrogenation [1] and tend to produce linear alkanes. Iron catalysts are more versatile than cobalt catalysts, produce less methane and can be geared for the production of alkenes, oxygenates and branched hydrocarbons depending on promoters and the process conditions employed [1-3]. Sasol is currently using an iron-based catalyst in a commercial slurry reactor; high alkene selectivity relative to fixed bed reactors is reported [6].

Several factors influence the selectivity and activity of FTS catalysts. Product selectivity of iron catalysts is generally controlled by promoting with one or more alkali metals [2]. Potassium has long been known to increase wax and alkene yields while decreasing the production of undesirable methane [2,7]. Potassium also has been implicated in increasing FTS and water-gas shift activity [8]. Activation procedures also can have a large affect on the selectivity and activity of iron catalysts [9,10]. Precipitated iron catalysts are generally activated with hydrogen, carbon monoxide or syngas. Catalysts activated with carbon monoxide have been reported to produce a higher molecular weight product than syngas or hydrogen activated catalysts; however,

several factors such as temperature, pressure and duration of the activation step determine the ultimate activity and stability of iron catalysts [10,11]; therefore, it is difficult to state which activation procedure is superior.

Copper has traditionally been added to precipitated iron catalysts to facilitate reduction of iron oxide to metallic iron during hydrogen activations [7]. Copper has been shown to minimize sintering of iron catalysts when activating with hydrogen by lowering the reduction temperature [2]. The effect of copper promotion on iron catalysts activated with carbon monoxide or syngas is not as well documented although Kölbel and Ralek have reported that only 0.1 wt% of copper is necessary for successful activation of Fe/Cu/K catalysts with syngas [5].

Throughout our FTS studies, it has been found that syngas activation at elevated pressure (>0.80 MPa) requires the catalyst be promoted with copper in order to achieve reasonable activity. Previous work in our laboratory has shown that the activity of syngas activated, Fe/Si/K catalysts is related to the hydrogen partial pressure of the activation gas [10]. Low hydrogen partial pressure inhibits the formation of oxidizing water which enables active iron carbides to be formed. Likewise, we have found that copper promotion has a similar effect. Treatment of a 100Fe/3.6Si/0.71K catalyst with syngas (H_2:CO=0.7) for 24 h at high pressure (1.31 MPa) and 270^{o}C resulted in syngas conversion below 18% [12]. When a 100Fe/3.6Si/2.6Cu/0.71K catalyst was treated similarly, the catalyst was found to undergo an induction period in which the syngas conversion increased to over 50% [12]. Mössbauer spectroscopy [12] analysis showed that the 100Fe/3.6Si/0.71K catalyst was composed of only Fe_3O_4 while the 100Fe/3.6Si/2.6Cu/0.71K catalyst had been partially carbided. The active species of iron-based Fischer-Tropsch catalysts has been debated since Fischer

initially proposed bulk carbides were responsible for catalyst activity [13]. Emmet later demonstrated that an iron catalyst carbided with ^{14}C labeled carbon monoxide produced hydrocarbons with a lower radioactivity than the catalyst, thereby indicating that the bulk carbide was not responsible for the activity; however, he did not rule out the possibility that a surface carbide could be responsible for FTS activity [14]. Biloen et al., using ^{13}C tracers, have proposed that a surface carbide species is responsible for FTS activity on nickel, cobalt and ruthenium catalysts [15]. Similarly, Stockwell et al. have proposed that a CH species derived from surface carbon is the active species on a supported iron catalyst [16]. Amelse et al. using Mössbauer spectroscopy [17] and more recently Shroff et al. using high resolution transmission electron microscopy [18] have proposed that the activity of iron catalysts is related directly to the extent of bulk carbide formation; however, these studies were conducted in fixed bed differential reactors at atmospheric pressure under low conversions and activity was based on the rate of methane formation. At low conversions, the H_2:H_2O and CO:CO_2 ratios are high enough that the reactor atmosphere is reducing and iron carbides are the thermodynamically stable phases [19]. At industrially relevant conditions, *i.e.*, high conversion, enough water and carbon dioxide are present to oxidize the catalyst. Mössbauer spectroscopy and X-ray diffraction of activated and used iron catalyst samples clearly indicate that iron carbides are oxidized to magnetite at high conversion at the bottom of fixed bed reactors [20]; however, fixed bed reactors are not ideal for conducting catalyst characterization studies, because at high conversion a reducing atmosphere exists at the entrance to the reactor while an oxidizing atmosphere (high H_2O and CO_2 partial pressure) may exist at the reactor outlet. We have conducted catalyst characterization studies in the slurry phase using continuous stirred tank

reactors [21,22]. In CSTR's all of the catalyst is exposed to the same reaction environment which allows for better correlation between catalyst composition and activity. We have found that a correlation between the amount of iron carbide and activity cannot always be made [22]; in some cases, peak catalyst activity is obtained when all of the bulk iron carbide appears to be oxidized to Fe_3O_4 [21].

Our research is currently directed at developing iron based catalysts for the production of wax and 1-alkenes from hydrogen-lean syngas. Herein we report results of the effect of activation gas (hydrogen, carbon monoxide or syngas) and promoters (potassium and copper) on the activity and selectivity of precipitated iron-silicon catalysts.

EXPERIMENTAL

Catalyst compositions are expressed as atomic percent relative to iron:

$$\frac{M}{M\%Fe} \; X \; 100$$

All catalysts used in this study were derived from a precipitated 100Fe/4.4Si/1.0K catalyst, unless otherwise noted. Preparation details of this catalyst are presented elsewhere [10]. Copper promotion was accomplished by impregnation with aqueous copper(II) nitrate hemipentahydrate. Additional potassium was added as potassium *tert*-butoxide during reactor loading. All FTS runs were conducted in a one liter autoclave operating as a continuous stirred tank reactor (CSTR) [10]. Catalysts were suspended in Ethylflo 164 hydrocarbon oil (Ethyl Corporation) which consists of a mixture of C_{30} isomers. All catalyst loadings were 10 or 5 weight percent. Hydrogen and carbon monoxide flow rates were controlled by two mass flow controllers (Brooks Instruments) with the resulting synthesis gas composition regulated by adjusting the

flow rate of the appropriate gas. The synthesis gas, after passing through a 2 L mixing vessel, was delivered to the catalyst slurry through a dip tube that extended below the impeller blade. The effluent exited the reactor and passed sequentially through two traps maintained at 60^{o}C and 0^{o}C. Accumulated reactor wax was removed daily through a tube fitted with a sintered metal filter (0.5-2.0 μm). Uncondensed effluent was sent to an on-line Carle gas analyzer for determination of carbon monoxide, hydrogen, carbon dioxide, methane and C_2-C_4 alkanes and alkenes. An on-line Hewlett-Packard 5790 GC equipped with a Porpack-Q column was utilized for C_4-C_9 quantification. Liquid samples were analyzed with a Hewlett-Packard 5890 GC equipped with a 60 m DB-5 capillary column. The reactor was also equipped with a tube that extended below the liquid level which permitted catalyst slurry samples to be withdrawn periodically.

Catalysts were activated with carbon monoxide, hydrogen or synthesis gas (H_2:CO=0.7). In general, the activation gas flow was started at ambient conditions, the necessary reactor pressure was set and the reactor was ramped to the appropriate temperature at 2^{o}C min^{-1}. After reaching the activation temperature, the conditions were maintained for 24 h. Carbon monoxide (2.0 NL h^{-1}g-Fe^{-1}) and syngas (3.4 NL h^{-1}g-Fe^{-1}) activations were conducted at 0.10 MPa and 270^{o}C while hydrogen (12 NL h^{-1}g-Fe^{-1}) activations were conducted at 0.10 MPa and 220^{o}C. The lower temperature and higher flow rate were chosen for the hydrogen activations in order to prevent sintering of the metallic iron that is formed [2]. Immediately following the activation procedure, reactors were brought to synthesis conditions: hydrogen:carbon monoxide ratio of 0.7, 3.1 NL h^{-1}g-Fe^{-1}(STP: 0^{o}C, 0.10 MPa), 230^{o}C or 270^{o}C , 1.31 MPa.

Thermogravimetric analyses (TGA) were performed with a Seiko SSC/5200 instrument. Each experiment was run with 20-30 mg of sample and a calcined alumina reference. Three different reducing gases were employed: 49% hydrogen in helium (195 mL min^{-1}), 39% carbon monoxide in helium (165 mL min^{-1}) and 47% syngas (H2:CO=0.7) in helium (190 mL min^{-1}). Samples were treated with the reducing gas at ambient conditions for 10 minutes and then the temperature was ramped to 600^{o}C (20^{o}C min^{-1}) and held for 5 minutes.

RESULTS AND DISCUSSION

Catalyst Activation

Previously reported results with 100Fe/3.6Si/0.73K and 100Fe/3.6Si/2.6Cu/0.73K catalysts clearly indicate that the formation of bulk carbide is necessary to obtain substantial activity and that copper plays a role in the carbide formation [12]. Thermogravimetric experiments have been performed to better explore the effects of copper on hydrogen, carbon monoxide and syngas activation of precipitated iron catalysts. Experiments were performed on a series of catalysts containing different quantities of copper (100Fe/4.4Si/5.2K, 100Fe/4.4Si/0.5Cu/5.2K, 100Fe/4.4Si/2.6Cu/5.2K, and 100Fe/4.4Si/5.0Cu/5.2K). Hydrogen reduction resulted in substantial weight loss with two inflections (Figure 1) that have been shown by Mössbauer spectroscopy and XRD [22] to correspond to the reduction sequence: Fe_2O_3 6 Fe_3O_4 6 Fe. Richard et al. [23] have reported similar findings with unpromoted and promoted Fe_2O_3 catalysts. Our results show the temperature where both reduction steps occur is dependent on the level of copper promotion. The onset of the reduction sequences shifted from ~250^{o}C and ~330^{o}C for the 100Fe/4.4Si/5.2K catalyst to ~200^{o}C and ~250^{o}C for the 100Fe/4.4Si/5.0Cu/5.2K catalyst (Figure 1).

Reduction with carbon monoxide produced two weight losses (Figure 2) corresponding to the sequential reduction of Fe_2O_3 to Fe_3O_4 and Fe_3O_4 to iron carbide(s) [22]. After the formation of iron carbide(s), a rapid weight gain corresponding to the deposition of Boudouard carbon was seen ($2CO\ 6\ C + CO_2$). Reduction with syngas (H_2:CO=0.7) gave results nearly identical to that found for carbon monoxide reduction (Figure 3). The similarity between carbon monoxide and syngas reduction is supported by Richard et al. who have reported that reduction of α-Fe_2O_3 with syngas (H_2:CO=1.0) is analogous to reduction with diluted carbon monoxide [23]. As was found with hydrogen reduction, the reduction steps for the carbon monoxide and syngas treated catalysts generally occurred at lower temperatures with increasing levels of copper.

It has been proposed that reduction of metal oxides to the zero valent state by hydrogen can be described by either a nucleation model or a contracting sphere model [24]. Only metal oxides that are reduced according to the nucleation mechanism have the reduction temperature affected by promoters, *i.e.* iron oxide promoted with copper. In the nucleation model, metal nuclei form by the removal of oxide ions from the lattice and the reduction process accelerates as previously formed nuclei grow and new nuclei are formed [24]. The reduction temperature of copper(II) oxide is approximately 150-200^{o}C lower than the reduction temperature of iron oxide. During the reduction of iron oxide promoted with copper oxide, the copper oxide will reduce to the metallic state first and will form sites of nucleation that accelerate the reduction of iron oxide [24]. Wachs et al. have studied the effects of copper and silver on the hydrogen reduction of low surface area α-Fe_2O_3 [25]. Copper was found to lower the temperature where reduction is initiated from ~300^{o}C to ~150^{o}C; however, promotion with silver had no

effect on the catalyst reduction. Copper was found to be much more dispersed on the catalyst surface than silver and was concluded to provide more sites of nucleation for reduction to occur. A similar process may occur for reduction with carbon monoxide or syngas. Shroff et al. have shown by transmission electron microscopy that reduction of a commercial iron oxide catalyst (Fe_2O_3/CuO/K_2O) with carbon monoxide proceeds by first reducing rapidly to Fe_3O_4 and then slowly to iron carbide(s) [18]. The iron carbide(s) were clearly shown to form as small nuclei on the surface of the Fe_3O_4 crystallites. Kölbel and Ralek report that only a small amount of copper is necessary to promote the reduction of iron oxide [5]. The results presented here show that the reduction with hydrogen, carbon monoxide or syngas is accelerated with increasing levels of copper promotion. This is in agreement with more nucleation sites being available with an increasing amount of copper.

Activity and Selectivity

We have developed a precipitated FT catalyst, 100Fe/4.4Si/1.0K, that shows high activity and stability [10]. With the proper activation, this catalyst has an initial carbon monoxide conversion greater than 90% and deactivates at a rate of 0.6% (CO conversion) per week when operating at 270^{o}C, 1.31 MPa, and a space velocity of 3.1 NL h^{-1}g-Fe^{-1} [10]. Activation with carbon monoxide (0.10 or 1.31 MPa) or syngas (H_2:CO=0.7, 0.10 MPa) at 270^{o}C results in carbon monoxide conversion above 90%; however, activations with hydrogen are only successful when the catalyst is promoted with copper (Figure 4). Carbon monoxide conversion of the 100Fe/4.4Si/1.0K catalyst activated with hydrogen started at 20% and gradually increased to ~60% during the first 600 h at synthesis conditions. In contrast, hydrogen activation of the same catalyst with copper promoter (100Fe/4.4Si/2.6Cu/1.0K) resulted in an initial carbon monoxide

conversion higher than 80%. This hydrogen activated catalyst showed stability equal to that of the carbon monoxide or syngas activated 100Fe/4.4Si/1.0K catalyst; a deactivation rate of less than 0.9% per week was achieved for over 3500 h. Bukur et al. have shown by XPS that carbon monoxide is more effective at reducing the surface of a commercial iron oxide catalyst promoted with copper, potassium and silica [26]. Richard et al. have shown that reduction of Fe_3O_4 to Fe_5C_2 by carbon monoxide is more thermodynamically favored than reduction of Fe_3O_4 to a-Fe by hydrogen [23]. As a result, copper promotion is necessary to ensure the formation of metallic iron when activating with hydrogen. High activity is then obtained when the metallic iron is converted to iron carbide(s) during synthesis.

We have generally found that catalysts activated with carbon monoxide have higher selectivity for high molecular weight products than catalysts activated with syngas or hydrogen [10]. Bukur et al. report carbon monoxide and syngas activations result in a heavier product distribution when a fixed bed reactor is used [21] while carbon monoxide activation results in lower methane selectivity than hydrogen or syngas activations in a slurry reactor [9]. However, all activation procedures using the 100Fe/4.4Si/1.0K catalyst resulted in a product distribution optimized for gasoline and light gases, not high value chemicals, *i.e.* wax and alkenes when FTS was conducted at 270^{o}C. Several factors are known to affect the selectivity of iron based catalysts in addition to the activation procedure. Alkali promotion, *i.e.* potassium has been well established as being critical for increasing alkene and wax yields while lowering the reaction temperature has been shown to decrease methane and increase wax production [2]. Increasing reaction pressure will also increase wax selectivity; however, it has been reported that catalyst stability decreases [9].

Since it is well known that decreasing FTS temperature and optimizing alkali promotion are effective at increasing wax and alkene yields, four low temperature runs were conducted at 230^{o}C on a 100Fe/4.4Si catalyst in which the potassium content was varied. The highest syngas conversion, after carbon monoxide activation, was obtained with a potassium loading between 4 and 5 atomic percent (Figure 5). Interestingly, at 270EC the maximum conversion for a similar catalyst was obtained with a potassium loading of ~1.0 atomic percent. Potassium is a FTS promoter because it increases the rate of dissociation of the C-O bond of carbon monoxide [27,28]. As the temperature is decreased it is harder to dissociate the C-O bond so a higher potassium loading is required. This is fortuitous, because the high potassium content needed at 230^{o}C also decreased methane and ethane production (Figure 5). Despite the improved selectivity, the activity of all of the 100Fe/4.4Si/xK catalysts were unacceptably low at 230^{o}C. The rate of hydrocarbon production relative to the amount of iron is a good measure of FTS activity. The rate of hydrocarbon production for a 100Fe/4.4Si/5.2K catalyst increased with respect to activation gas according to the order: hydrogen < syngas < carbon monoxide. The activity of the carbon monoxide activated catalyst underwent an induction period in which the rate of hydrocarbon production reached 0.30 g h^{-1}g-Fe^{-1} after 72 h (Figure 6). The hydrogen activated catalyst also went through an induction period; however, the activity was less than half that obtained when activation was conducted with carbon monoxide (Figure 6). The syngas activated catalyst deactivated slowly from a maximum rate of 0.24 g h^{-1}g-Fe^{-1} (Figure 6).

Bukur et al. have reported that copper promotion increases FTS activity of precipitated iron catalysts and that there is a synergistic effect when both potassium

and copper are used [8]. Soled et al. have claimed promotion with both potassium and copper is essential to obtain the highest activity, lowest methane selectivity and highest alkene selectivity with a precipitate iron-zinc catalyst [29]. In an effort to improve FTS activity at 230^{o}C, the 100Fe/4.4Si/5.2K catalyst was promoted with copper to give a composition of 100Fe/4.4Si/2.6Cu/5.2K. It was found that copper promotion significantly increased FTS activity for the carbon monoxide, syngas and hydrogen activated catalysts (Figure 6). The maximum rate of hydrocarbon production achieved with the different activation gases increased in the order: hydrogen (0.25) < carbon monoxide (0.38) < syngas (0.43 g h^{-1}g-Fe^{-1}). Maximum syngas conversion followed similar trends; hydrogen (38%) < carbon monoxide (56%) < syngas (64%) (Figure 7).

Carbon dioxide selectivity was found to be higher for the catalyst with copper (Figure 8) which indicates that copper is a promoter for the water-gas shift reaction. Carbon dioxide selectivity obtained for the 100Fe/4.4Si/2.6Cu/5.2K catalyst varied according to the activation gas as follows: carbon monoxide < syngas < hydrogen (Figure 9). Bukur et al. also report that hydrogen activation leads to higher water-gas shift activity when operating at 260EC [9].

Product selectivities for the 100Fe/4.4Si/5.2K and 100Fe/4.4Si/2.6Cu/5.2K catalysts are shown in Table 1. Methane selectivity was low and wax selectivity was high for all runs. The best overall performance, based on syngas conversion and selectivity, was achieved by the syngas activated 100Fe/4.4Si/2.6Cu/5.2K catalyst. This is unlike the runs made at 270EC with the 100Fe/4.4Si/1.0K catalyst which had similar activity when activated with carbon monoxide or syngas. Methane selectivity less than 3 wt% (based on total hydrocarbon product), wax selectivity greater than 70 wt% and high alkene yields were obtained at moderately high carbon monoxide

conversion (>60%). The syngas activated 100Fe/4.4Si/2.6Cu/5.2K catalyst showed reasonable stability with total conversion greater than 50% maintained for over 300 h. Contrary to FTS activity, alkene selectivity is not appreciably affected by the activation gas or the presence of copper. Alkene selectivity for the C_2-C_{11} product fraction was typically above 70 wt%. Much interest of the commercial viability of iron based FTS catalysts has focused on their ability to produce 1-alkenes for chemical feedstocks. We have found that over 95% of the alkene fraction is composed of 1-alkenes for the 100Fe/4.4Si/xCu/5.2K catalysts (x=0 or 2.6) when FTS is conducted at 230^{o}C . Table 1 shows the selectivity of the C_2-C_{11} 1-alkenes, relative to the total FTS product. Although geared for the production of wax and transportation fuels, the 100Fe/4.4Si/2.6Cu/5.2K catalyst also produces significant amounts of light alkenes, in fact, ethylene and propylene and 1-butene are the most abundant of all products by mass.

CONCLUSIONS

Moderately high FTS activity has been achieved in the slurry phase under industrially relevant conditions with a precipitated iron-silicon catalyst at 230^{o}C. Optimum potassium promotion for a 100Fe/4.4Si/xK catalyst is in the range of 4-5 atomic %, relative to iron. In general, syngas and carbon monoxide activations at 270^{o}C and 0.10 MPa result in better catalyst performance than hydrogen activation at 220^{o}C. Low methane and high wax and alkene selectivities have been achieved for 100Fe/4.4Si/xCu/5.2K catalysts (x=0 or 2.6).

The major difference between running at 270^{o}C and 230^{o}C has been a rapid deactivation after approximately 300 h on stream for the 230^{o}C runs. Work in progress suggests that the deactivation is linked to the difficulty of separating the catalyst from

the heavy wax that accumulates in the reactor. Eventually all of the runs reported here were stopped because the reactors had become filled with wax soon after plugging of the internal filter. Work in progress has shown a lower catalyst loading (<5 wt%) to reduce wax production has enabled us to run for longer times and verify that the 100Fe/4.4Si/2.6Cu/5.2K catalyst is stable for over 500 h. A study of catalyst deactivation will be reported elsewhere.

Copper promotion has been found to be imperative for low temperature FTS or when hydrogen activations are utilized. Hydrocarbon productivity increased by as much as a factor of two with copper promotion. Copper has been found to increase the activity of hydrogen activated catalysts by lowering the reduction temperature which in turn reduces sintering of the metallic iron that is formed [2]. However, this does not explain why FTS activity of carbon monoxide and syngas activated catalysts is increased dramatically by copper promotion. Carbon monoxide and syngas activation generally reduce iron oxide catalysts to a mixture of iron carbides which are not as susceptible to sintering as metallic iron. Thermogravimetric analyses clearly show that copper lowers the reduction temperature of hydrogen, carbon monoxide and syngas treated catalysts. In addition, it has been found that the temperature of the reduction onset is correlated with the amount of copper. Based on previous reports, it can be speculated that increasing copper content increases the number of nucleation sites for the reduction process [25].

The FTS reaction requires a 2:1 hydrogen:carbon monoxide ratio, so catalysts must have good water-gas shift activity if syngas with low levels of hydrogen is used, *i.e.* H_2:CO=0.7. One possibility for the increase in FTS activity we observe with copper promotion is that copper increases the water-gas shift activity. This is consistent with

copper being used in commercial low temperature water-gas shift catalysts. We have also found that copper promotion appears to favor the formation of iron carbides [12]. It may be possible that copper increases the activity of iron catalysts by increasing the number of active sites that are formed. Assuming that the active site(s) is a zero valent surface species, copper may serve as a means of preventing oxidation of the active metallic iron or iron carbide.

REFERENCES

[1] G. A. Mills, Catalysts for Fuels from Syngas, IEA Coal Research, London, 1988, pp. 34-44.

[2] M. E. Dry, in J. R. Anderson and M. Boudart (Editors), Catalysis Science and Technology, Vol. 1, Springer-Verlag, New York, 1981, p. 159.

[3] M. E. Dry, Proc. S. African Catal. Soc. Catalysis and Catalytic Processes, Oct. 1993.

[4] V. U. S. Rao, G. J. Stiegel, G. J. Cinquegrane and R. D. Srivastava, *Fuel Processing Technology*, 30 (1992) 83.

[5] H. Kölbel and M. Ralek, *Catal. Rev.-Sci. Eng.*, 21 (1980) 225.

[6] B. Jager and R. Espinoza, *Catal. Today*, 23 (1995) 17.

[7] H. Storch, N. Golumbic and R. B. Anderson, Fischer-Tropsch and Related Synthesis, Wiley, New York, 1951.

[8] D. B. Bukur, D. Mukesh, and S. A. Patel, *Ind. Eng. Chem. Res.*, 29 (1990) 194.

[9] D. B. Bukur, L. Nowicki, and X. Lang, *Energy & Fuels*, 9 (1995) 620.

[10] R. J. O'Brien, L. Xu, R. L. Spicer and B. H. Davis, accepted by *Energy & Fuels*.

[11] D. B. Bukur, X. Lang, J. A. Rossin, W. H. Zimmerman, M. P. Rosynek, E. B. Yeh and C. Li, *Ind. Eng. Chem. Res.*, 28 (1989) 1130.

[12] K. R. P. M. Rao, F. E. Huggins, G. P. Huffman, R. J. Gormley, R. J. O'Brien and B. H. Davis, Energy & Fuels, 10 (1996) 546.

[13] F. Fischer and H. Tropsch, *Ges. Abhandl. Kenntnis Kohle*, 10 (1932) 313.

[14] J. T. Kummer, T. W. Dewitt and P. H. Emmet, *J. Am. Chem. Soc.*, 70 (1948) 3632.

[15] P. Biloen, J. N. Helle and W. M. H. Sachtler, *J. Catal.*, 58 (1979) 95.

[16] D. M. Stockwell, D. Bianchi and C. O. Bennet, *J. Catal.*, 113 (1988) 13.

[17] J. A. Amelse, J. B. Butt and L. H. Schwartz, *J. Phys. Chem.*, 82 (1978) 558.

[18] M. D. Shroff, D. S. Kalakkad, K. E. Coulter, S. D. Köhler, M. S. Harrington, N. B. Jackson, A. G. Sault and A. K. Datye, *J. Catal.*, 156 (1995) 185.

[19] G. L. Vogler, X.-Z. Jiang, J. A. Dumesic and R. J. Madon, *J. Catal.*, 89 (1984) 116.

[20] D. B. Bukur, M. K. Koranne, X. Lang, K. R. P. M. Rao and G. P. Huffman, *Applied Catal.*, 126 (1995) 85.

[21] C. S. Huang, B. Ganguly, G. P. Huffman, F. E. Huggins and B. H. Davis, *Fuel Sci. Technol. Int.*, 11 (1993) 1289.

[22] R. J. O'Brien, L. Xu, D. R. Milburn, Y.-X. Li, K. J. Klabunde and B. H. Davis, *Topics in Catalysis*, 2 (1995) 1.

[23] M. A. Richard, S. L. Soled, R. A. Fiato and B. A. DeRites, *Mat. Res. Bull.*, 18 (1983) 829.

[24] N. W. Hurst, S. J. Gentry and A. Jones, *Catal. Rev.-Sci. Eng.*, 24 (1982) 233.

[25] I. E. Wachs, D. J. Dwyer and E. Iglesia, *Applied Catal.*, 12 (1984) 201.

[26] D. B. Bukur, K. Okabe, M. P. Rosynek, C. Li, D. Wang, K. R. P. M. Rao and G. P. Huffman, *J. Catal.*, 155 (1995) 353.

[27] M. E. Dry, T. Shingles, L. J. Boshoff and G. J. Oosthuizen, *J. Catal.*, 15 (1969) 190.

[28] J. Benzinger and R. J. Madix, *Surface Sci.*, 94 (1980) 119.

[29] S. L. Soled, S. Miseo, E. Iglesia and R. A. Fiato, U.S. Pat., 5,100,856 (1992).

Table 1

Selectivity of 230°C FTS Runs

Activation Gas	H_2		CO		H_2:CO = 0.7	
Catalyst[a]	I	II	I	II	I	II
TOS/h	168	168	168	192	624	192
Conversion/mol %						
CO	17	35	40	39	25	68
H_2	17	31	42	38	22	58
CO + H_2	17	34	41	39	24	64
Water-Gas Shift						
H_2:CO Usage	0.69	0.60	0.73	0.68	0.64	0.60
K_p[b]	4	9	3	4	4	11
CO_2 selectivity/%, C basis	44	42	43	42	44	45
Productivity						
Total HC/gm^{-3} feed	35	71	83	84	51	138
C_3 + HC/gm^{-3} feed	33	65	78	79	45	130
C_3+ HC/gm^{-3} converted	194	191	190	202	188	203
Total HC/g h^{-1}g-Fe^{-1}	0.10	0.22	0.25	0.26	0.15	0.42
Selectivity/wt.%[c]						
C_1	2.6	3.8	2.9	2.2	5.7	2.2
C_2-C_4 (alkene)[d]	10	14(72)	15(82)	12(80)	21(79)	11(77)
C_5-C_{11} (alkene)[d]	20	37(66)	27(78)	25(76)	34(75)	15(78)
C_{12}+	67	44	55	60	39	72
1-alkene/wt.%[c]						
C_2	2.0	2.9	3.4	2.6	5.2	2.5
C_3	2.8	4.1	4.9	3.9	6.4	3.4
C_4	2.2	3.2	3.8	3.2	4.4	2.1
C_5	1.8	4.2	3.1	2.6	4.8	2.3
C_6	2.1	3.2	3.0	2.6	3.9	1.4
C_7	1.4	2.4	2.9	2.1	4.1	1.3
C_8	1.3	2.2	2.3	2.2	2.8	1.2
C_9	0.96	2.5	1.9	1.9	2.8	1.2
C_{10}	1.2	2.2	1.6	1.6	2.0	1.1
C_{11}	1.2	2.1	1.4	1.6	1.9	1.1

a. I, 100 Fe/4.4 Si/5.2 K; II, 100 Fe/4.4 Si/2.6 Cu/5.2 K

b. $K_p' (p_{CO_2} p_{H_2})/(p_{CO} p_{H_2O})$

c. Based on total hydrocarbon product

d. Wt.% of hydrocarbon fraction

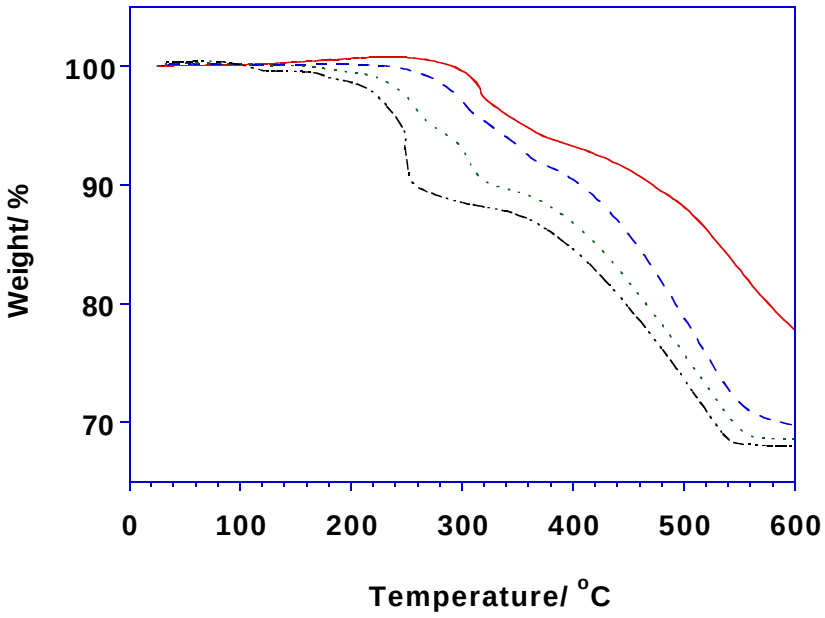

Figure 1. Weight change measured by thermogravimetric analysis of 100Fe/4.4Si/5.2K (—), 100Fe/4.4Si/0.5Cu/5.2K (– – –), 100Fe/4.4Si/2.6Cu/5.2K (·····) and 100Fe/4.4Si/5.0Cu/5.2K (—··—) catalysts reduced with hydrogen.

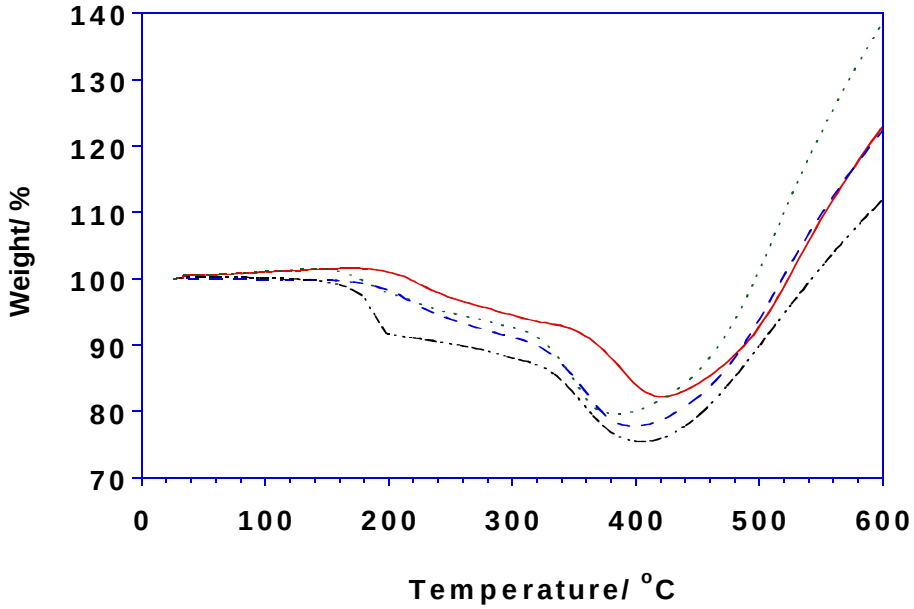

Figure 2. Weight change measured by thermogravimetric analysis of 100Fe/4.4Si/5.2K (—), 100Fe/4.4Si/0.5Cu/5.2K (– – –), 100Fe/4.4Si/2.6Cu/5.2K (·····) and 100Fe/4.4Si/5.0Cu/5.2K (—··—) catalysts reduced with carbon monoxide.

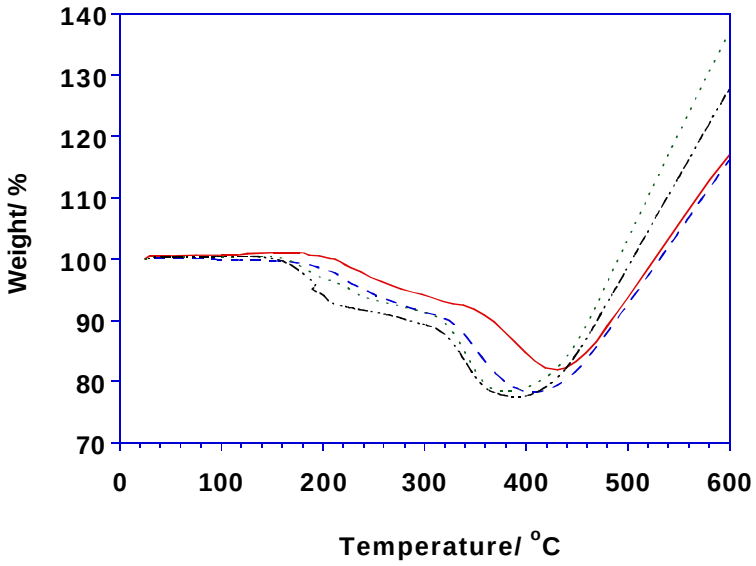

Figure 3. Weight change measured by thermogravimetric analysis of 100Fe/4.4Si/5.2K (—), 100Fe/4.4Si/0.5Cu/5.2K (– – –), 100Fe/4.4Si/2.6Cu/5.2K (·····) and 100Fe/4.4Si/5.0Cu/5.2K (—··—) catalysts reduced with syngas (H_2:CO=0.7).

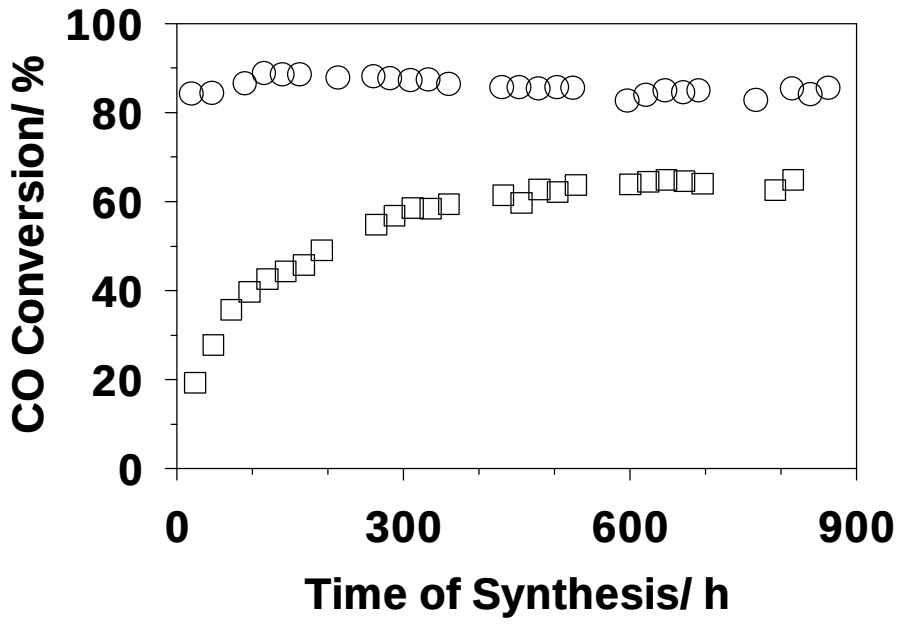

Figure 4. Carbon monoxide conversion as a function of time on stream for a 100Fe/4.4Si/1.0K catalyst (**G**) and a 100Fe/4.4Si/2.6Cu/1.0K catalyst (**F**). Activation conditions: H_2 flow rate=12 NL h^{-1}g-Fe^{-1}, 220°C, 0.10 MPa, 24 h. Synthesis conditions: H_2:CO=0.7, 3.1 NL h^{-1}g-Fe^{-1}, 270°C, 1.31 MPa.

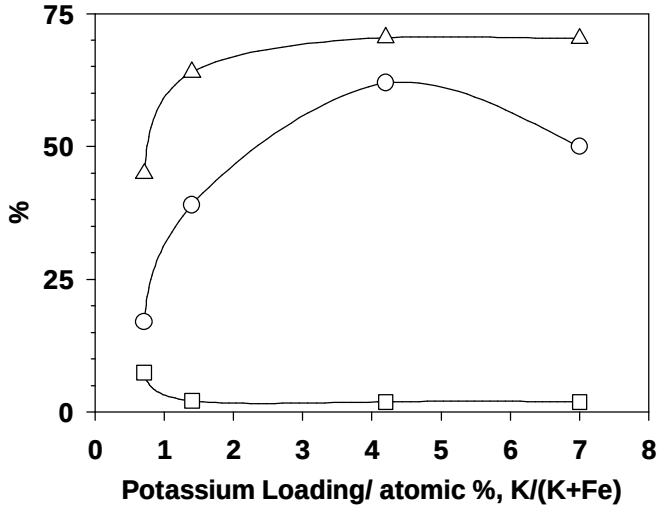

Figure 5. Syngas conversion (**F**), C_2-ethylene selectivity ([a]) and methane selectivity, wt% of hydrocarbon product (**G**) as a function of potassium loading for a 100Fe/4.4Si catalyst. Synthesis conditions: H_2:CO=0.7, 1.0 NL h^{-1}g-Fe^{-1}, 230°C and 1.31MPa.

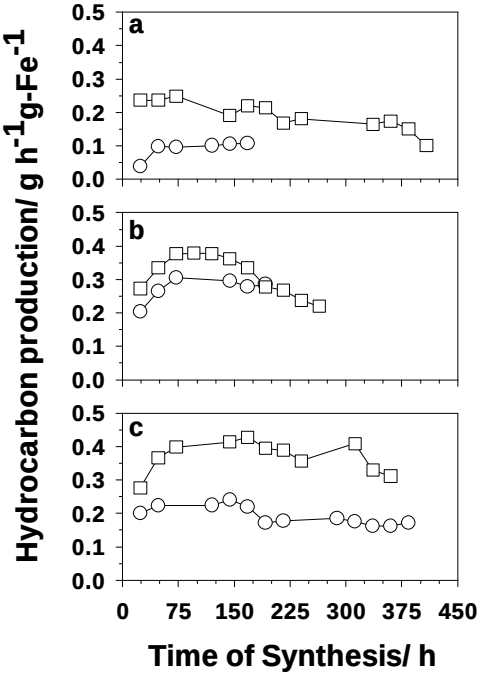

Figure 6. Hydrocarbon production rate for 100Fe/4.4Si/5.2K (**F**) and 100Fe/4.4Si/2.6Cu/5.2K (**G**) catalysts. Activation conditions: (a) hydrogen flow rate=12 NL h^{-1}g-Fe^{-1}, 220°C, 0.10 MPa for 24 h, (b) carbon monoxide flow rate =2.0 NL h^{-1}g-Fe^{-1}, 270°C, 0.10 MPa for 24 h, (c) H_2:CO=0.7 at 3.1 NL h^{-1}g-Fe^{-1}, 270°C, 0.10 MPa for 24 h. Synthesis conditions: H_2:CO=0.7, 3.1 NL h^{-1}g-Fe^{-1}, 230°C and 1.31MPa.

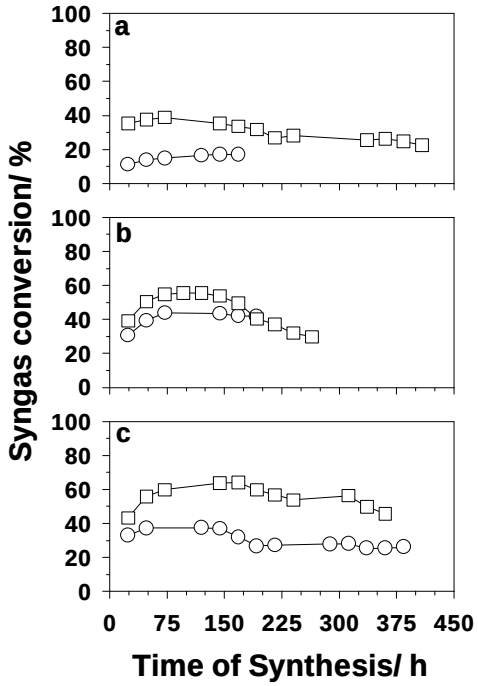

Figure 7. Syngas conversion for 100Fe/4.4Si/5.2K (**F**) and 100Fe/4.4Si/2.6Cu/5.2K (**G**) catalysts. Activation conditions: (a) hydrogen flow rate=12 NL h^{-1}g-Fe^{-1}, 220°C, 0.10 MPa for 24 h, (b) carbon monoxide flow rate =2.0 NL h^{-1}g-Fe^{-1}, 270°C, 0.10 MPa for 24 h, (c) H_2:CO=0.7 at 3.1 NL h^{-1}g-Fe^{-1}, 270°C, 0.10 MPa for 24 h. Synthesis conditions: H_2:CO=0.7, 3.1 NL h^{-1}g-Fe^{-1}, 230°C and 1.31MPa.

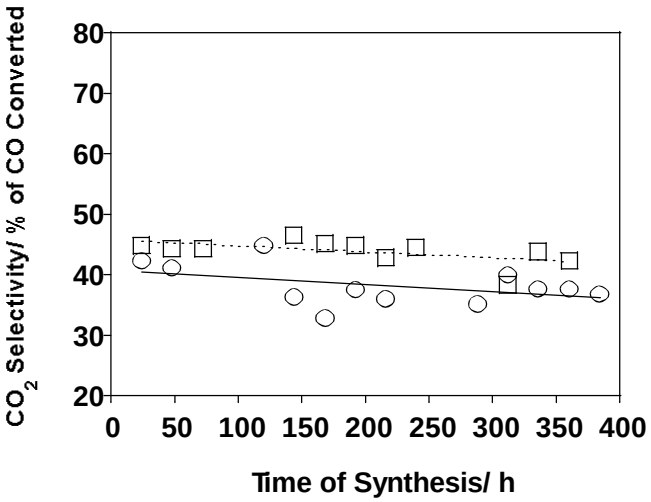

Figure 8. Carbon dioxide selectivity for 100Fe/4.4Si/5.2K (**F**) and 100Fe/4.4Si/2.6Cu/5.2K (**G**) catalysts. Activation conditions: H_2:CO=0.7 at 3.1 NL h^{-1}g-Fe^{-1}, 270°C, 0.10 MPa for 24 h. Synthesis conditions: H_2:CO=0.7, 3.1 NL h^{-1}g-Fe^{-1}, 230°C and 1.31MPa.

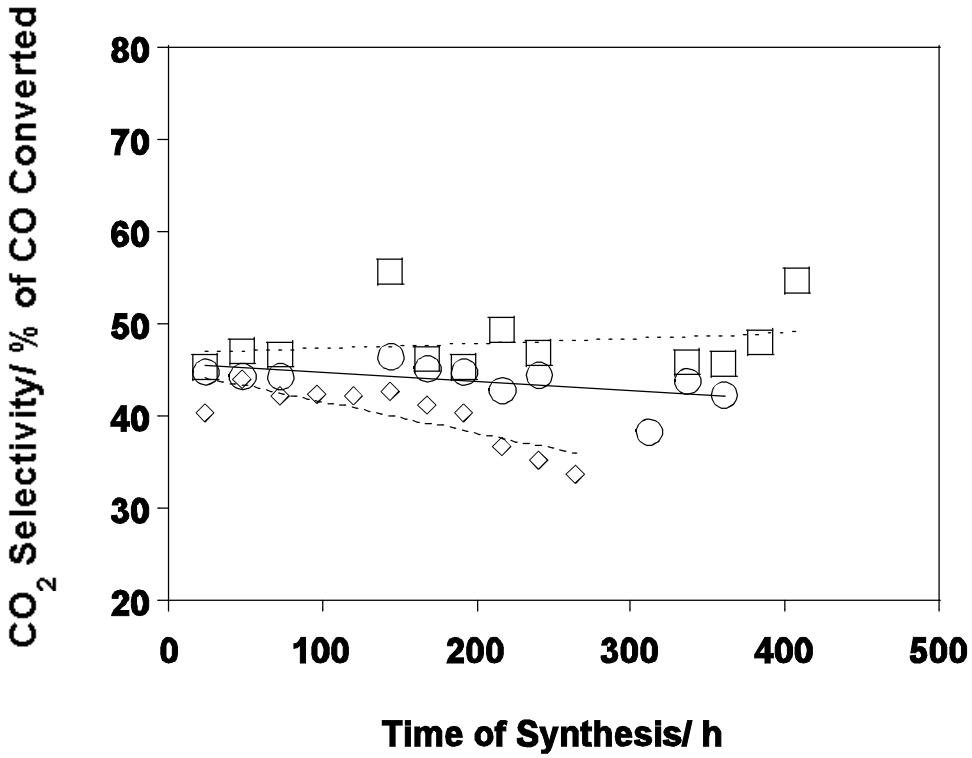

Figure 9. Carbon dioxide selectivity for 100Fe/4.4Si/2.6Cu/5.2K catalyst activated with hydrogen (**G**), syngas (H_2:CO=0.7) (**F**) and carbon monoxide (•). Synthesis conditions: H_2:CO=0.7, 3.1 NL h^{-1}g-Fe^{-1}, 230°C and 1.31MPa.

3.1.2 Effect of Potassium Promotion on Iron-Based Catalysts For Fischer-Tropsch Synthesis

ABSTRACT

The effect of potassium on catalyst activity, kinetic parameters and selectivity has been investigated for a precipitated iron catalyst that was employed with low H_2/CO ratio typical of a synthesis gas generated from coal. A wide range of synthesis gas conversions have been obtained by varying space velocities over catalysts with various potassium loadings. Differing trends in catalyst activity with potassium loading were observed depending on the space velocity or synthesis gas conversion. As potassium loading increased, the catalyst activity either decreased (low conversions), passed through a maximum (intermediate conversions) or increased (high conversions). This is shown to be a result of the increasing dependency of the Fischer-Tropsch synthesis on the hydrogen formed by the water-gas shift reaction with increasing synthesis gas conversions. Both the rate constant and the adsorption parameter in a common two-parameter Fischer-Tropsch rate expression decreased with potassium loading; therefore, observed maxima in Fischer-Tropsch rate with potassium loading can be due to the opposing influences of these parameters. The effect of potassium on alkene selectivity was dependent on the number of carbon atoms of the hydrocarbons as well as the carbon monoxide conversion level. The extent of isomerization of alkene products decreased with potassium loading, while the selectivity to methane decreased with increasing potassium content at CO conversions about 50% and higher.

INTRODUCTION

The Fischer-Tropsch Synthesis (FTS) converts synthesis gas, a mixture of carbon monoxide and hydrogen, to hydrocarbons. The FTS reaction can be represented as:

$$CO + (1+(n/2))\ H_2 \rightarrow CH_n + H_2O \quad \textbf{(1)}$$

where n is the average H/C ratio of the hydrocarbons produced. Iron-based catalysts possess activity for the water gas shift (WGS) reaction. This property allows the direct processing of synthesis gas with a low H_2/CO ratio (as produced by coal gasification in advanced gasifiers) without an additional WGS reactor. The WGS reaction provides the extra hydrogen needed for the FTS.

$$CO + H_2O \rightarrow CO_2 + H_2 \quad \textbf{(2)}$$

Typical iron-based catalysts contain small amounts of potassium along with binders such as silica or alumina. The role of potassium on iron-based catalysts has been previously studied; however, the results of the effect of potassium on catalyst activity vary considerably with different researchers, different temperatures and with the presence/amount of binders used (1-4). Potassium has been shown to increase catalytic activity (1, 2, 4), decrease activity (2, 3), and in some cases the activity has been shown to reach a maximum with increasing potassium loading and then decline with further addition of potassium (1, 2). Further, systematic studies of possible reasons for catalyst activity trends have rarely been performed.

A reaction rate expression proposed (5) for the FTS is

$$-r_{CO+H_2} = \frac{kP_{CO}P_{H_2}^2}{P_{CO}P_{H_2} + bP_{H_2O}} \quad \textbf{(3)}$$

Based on this rate expression, changes in catalyst FTS activity could be due to changes in: (i) rate constant, k, (ii) adsorption parameter, b, and (iii) partial pressure of water. In addition, the rate and extent of the WGS reaction has a major effect on the FTS activity, especially for a low H_2/CO ratio synthesis gas. Studies of the effect of potassium loading on the kinetic parameters of the Fischer-Tropsch Synthesis or the effect of the WGS reaction on the FTS activity have not been previously reported in detail.

Addition of potassium has been found to affect the catalyst selectivity. Potassium apparently increases the alkene content of the hydrocarbon products, increases the rate of the WGS reaction and suppresses methane formation. However, these selectivity comparisons have often been made at different synthesis gas conversion levels (3, 4). It is known that selectivity changes with synthesis gas conversion and thus a comparison at equal conversion levels would be more appropriate to discern selectivity changes (6).

In this study, a systematic comparison of the effect of increasing potassium levels on iron-based catalyst activity and selectivity is conducted. Data were obtained for each potassium level over a wide range of synthesis gas conversions by varying feed space velocities. Thus, the effect of potassium on kinetic parameters has been determined and selectivity comparisons made at equal conversion levels. An attempt is made to discern the reason(s) for changes in catalyst activity with increasing potassium levels.

EXPERIMENTAL

Catalysts

The base catalyst used was a precipitated iron-silica catalyst with atomic ratio 100Fe/4.6Si. The preparation of this catalyst using a continuous precipitation procedure has been described previously (7). Various levels of potassium were added by incipient wetness impregnation with aqueous potassium nitrate. Final catalyst compositions in atomic ratio were: 100Fe/4.6Si/0.36K, 100Fe/4.6Si/1.4K and 100Fe/4.6Si/2.2K.

Reaction System

A 1-liter autoclave operated as a continuous stirred tank reactor (CSTR) was used for the slurry FTS reactions. Analysis of the gaseous, liquid and solid (at room temperature) products was conducted both on- and off-line using a variety of gas chromatographs. More details of the reaction system used and product analysis have been reported previously (8).

Procedure

Approximately 5 g of catalyst was mixed with 300 g of melted octacosane (purified to remove halogens) in the CSTR. The reactor pressure was increased to 13.1 MPa with carbon monoxide at a flow rate of 13 NL h^{-1} (20°C, 0.10 MPa). The reactor temperature was increased to 270°C at a rate of 120°C h^{-1}. These activation conditions were maintained for 24 h.

At the end of the activation period, synthesis gas flow was started at a H_2/CO ratio of 0.67. During the entire run the reactor temperature was 270°C, the pressure was 13.1 MPa and the stirring speed was maintained at 750 rpm. About two days were required before the catalyst reached steady state as evidenced by the constant

conversion of synthesis gas. Subsequently, the space velocity of the synthesis gas was varied between 5 and 65 NL h^{-1} g-Fe^{-1}. The conversions of carbon monoxide, hydrogen, and the formation of various products were measured with a period of approximately 24 hours at each space velocity. The H_2/CO ratio of the feed synthesis gas was kept constant at 0.67 at all the space velocities. Periodically during the run, the catalyst activity was measured at pre-set ?standard" conditions (a space velocity of 10 NL h^{-1} g-Fe^{-1}) to check for catalyst deactivation.

RESULTS

The results for three potassium levels (0.36, 1.4 and 2.2) are presented. Representative runs for the 0.36 K and 1.4 K catalysts lasted for 500 hours during which the catalyst activity was constant as measured at pre-set ?standard" conditions. Preliminary data for the 2.2 K catalyst showed that this catalyst deactivated after about 250 hours of time on stream. Hence, data for this catalyst were obtained in multiple runs lasting for a maximum of 250 hours. The synthesis gas conversion as measured in multiple runs was accurate to about +/- 1.5%.

Conversions

The syngas conversion is a rough measure of the overall Fischer-Tropsch activity of an iron-based catalyst. The syngas conversion for the three levels of potassium studied is shown in Figure 1. It is immediately evident that the trends in synthesis gas conversion with potassium loading are dependent on the space time (reaction time) or the conversion level. At low synthesis gas conversion levels or low space times, the catalyst with the lowest potassium loading (0.36 K) exhibited the highest synthesis gas conversion. At intermediate conversion levels, the catalyst with an intermediate potassium loading (1.4 K) exhibited the highest synthesis gas

conversion. At the highest conversion levels, the synthesis gas conversion exhibited by all three of the catalysts closely approached each other.

This is more clearly shown in Figure 2 where the synthesis gas conversion is plotted against potassium loading at various space velocities. At high space velocities, potassium appears to act as a catalyst poison. At the lowest space velocities, potassium appears to slightly enhance the synthesis gas conversion. At intermediate space velocities, there appears to be an optimum potassium level for maximum synthesis gas conversion.

The same trends obtained for synthesis gas conversion are also evident for the hydrocarbon production rate with potassium loading (Figure 3). This confirms that synthesis gas conversion is a good measure of the overall FTS activity.

Product/Reactant Partial Pressures

The partial pressure of water is an important parameter in the FTS. Water has been shown to inhibit the FTS reaction rate (Equation 3). As shown in Figure 4, the partial pressure of water in the reactor exhibits the behavior of a reaction intermediate, i.e., the water partial pressure is high initially and then decreases with reaction time. This is not surprising as the water formed by the FTS can be subsequently consumed in the WGS reaction. In general, the partial pressure of water in the reactor decreases with potassium loading.

The reaction rate expression given in Equation (3) can be rearranged as

$$\&4_{CO\%H_2} \; ' \; \frac{kP_{H_2}}{1 \; \% \; b\left(\frac{P_{H_2O}}{P_{CO}P_{H_2}}\right)} \qquad \textbf{(4)}$$

In contrast to the water partial pressure, the value of the partial pressure ratio,

$$\frac{P_{H_2O}}{P_{CO}P_{H_2}}$$

increases monotonically with reaction time as shown in Figure 5. The value of the partial pressure ratio increases, in general, with potassium loading.

Reaction Rates of FTS and WGS

The individual rates of reaction of the FTS (r_{FTS}) and WGS (r_{WGS}) can be calculated from experimentally observed quantities by:

$$r_{WGS} = r_{CO_2} \quad \textbf{(5)}$$

and

$$r_{FTS} = r_{CO} - r_{CO_2} \quad \textbf{(6)}$$

where r_{CO_2} is the rate of carbon dioxide formation and r_{CO} is the rate of carbon monoxide conversion.

These calculated rates of the two reactions are shown in Figure 6 for the three potassium levels. At low reaction times, the rate of the FTS is much greater than the rate of the WGS reaction; however, the rate of the WGS reaction closely approaches the rate of the FTS at high reaction times. The trends in the FTS rate at different potassium loadings are similar to the variation of synthesis gas conversions with potassium loading (Figure 1).

At low reaction times, there are marked differences between the WGS reaction rates for different potassium loadings. The catalyst with intermediate potassium loading (1.4 K) exhibits the highest WGS reaction rate at the low reaction times;

however, at high reaction times the rates of the WGS for the three potassium loadings are quite similar.

Extent of WGS

One measure of the extent of the WGS reaction can be obtained by following the WGS reaction quotient (RQ_{WGS}).

$$RQ_{WGS} = \frac{P_{CO_2} P_{H_2}}{P_{CO} P_{H_2O}} \quad \textbf{(7)}$$

As shown in Figure 7, the value of the reaction quotient is small at low carbon monoxide conversions and increases considerably at higher carbon monoxide conversions. The value of the reaction quotient increases with potassium loading at the same carbon monoxide conversions. Hence, the extent of the WGS reaction measured in this way appears to increase with potassium loading.

The FTS reaction produces water which is a necessary reactant for the WGS reaction to proceed. Thus the rate/extent of the WGS reaction is limited by the amount of water formed by the FTS. Since water is not supplied to the reactor, the stoichiometry of the FTS and WGS reactions (Equations (1) and (2)) dictates that

$$r_{WGS} < or = r_{FTS} \quad \textbf{(8)}$$

Hence, a more reliable measure of the extent of the WGS reaction is to compare the relative rate of the WGS to the rate of the FTS to see how closely the rate of the WGS approaches that of the FTS. As shown in Figure 8, the ratio of the FTS rate to the WGS reaction rate increases with carbon monoxide conversion and approaches a value of one. This is consistent with the data shown in Figures 6 and 7. Figure 8

clearly shows that the extent of the WGS reaction increases substantially with potassium loading at carbon monoxide conversions less than 80%. However, at high carbon monoxide conversions the increase in the extent of the WGS reaction with potassium loading is small.

Kinetics

The reaction rate expression given in Equation (3) can be linearized by rearrangement as

$$\frac{P_{H_2}}{-r_{CO+H_2}} = \frac{1}{k} + \frac{b}{k}\frac{P_{H_2O}}{kP_{CO}P_{H_2}} \qquad \textbf{(9)}$$

Hence a plot of $\frac{P_{H_2}}{-r_{CO+H_2}}$ versus $\frac{P_{H_2O}}{P_{CO}P_{H_2}}$ should give a straight line whose intercept is given by (1/k) and whose slope is given by (b/k).

The data for the three potassium loadings studied are plotted in this manner in Figure 9. It is evident that the results do not lie on a single straight line for any of the catalysts studied. The regression lines shown in Figure 9 have been drawn through the data obtained at low conversions. This situation is analyzed in the Discussion section.

Alkene Selectivity

Figure 10 illustrates the alkene selectivity of the light hydrocarbon products (C_2 and C_3) obtained. Both the C_2 and C_3 alkene selectivities decrease with carbon monoxide conversion for all the catalysts studied. The selectivity to C_2 alkene increases with potassium loading at similar carbon monoxide conversions. This is true over the entire range of carbon monoxide conversions obtained in this study. However, the effect of increasing potassium amounts on the selectivity to C_3 alkenes depends on

the carbon monoxide conversion level; at lower carbon monoxide conversions the highest alkene selectivity is obtained over the 0.36 K catalyst, while at higher conversions the highest alkene selectivity is exhibited by the 1.4 K and 2.2 K catalysts.

1-Alkene Selectivity

The isomerization ability at different potassium levels can be compared from the selectivity of the 1-alkene relative to the total alkenes (1-alkene + cis-2-alkene + trans-2-alkene) produced. This is illustrated for the butenes in Figure 11 for the three potassium levels as a function of carbon monoxide conversion. The selectivity to 1-butene decreases with increasing carbon monoxide conversion and increases with increasing potassium loading at similar carbon monoxide conversions.

Methane Selectivity

As shown in Figure 12, the methane selectivity was constant and similar for all the catalysts studied at low carbon monoxide conversions. Above 50% carbon monoxide conversion, the methane selectivity increased with increasing conversion. The selectivity to methane increased with decreasing potassium loading.

DISCUSSION

Effect of Increase in Potassium on WGS and FTS

For synthesis gas with a low H_2/CO ratio, the extent and/or rate of the WGS is extremely important to achieve a high conversion of carbon monoxide. For example, if there was no WGS, then according to Equations (1) and (2) the maximum carbon monoxide conversion would be 31%, assuming n = 2.3 (actual values of n or the average H/C ratio of the hydrocarbon products are between 2.2 and 2.4). In the case of all three of the catalysts studied, there is always some accompanying WGS reaction. In order to illustrate the importance of a high WGS reaction rate, it is necessary to

calculate the rate of hydrogen consumed by the FTS reaction. This can be calculated from the stoichiometry of the FTS (Equation 1) as

$$H_2 \ consumed \ by \ FTS \ ' \ r_{FTS}(1\%(n/2)) \qquad \textbf{(10)}$$

Figure 13 shows a comparison of the hydrogen consumed by the FTS and the hydrogen supplied to the reactor for the three potassium loadings as a function of reaction time. The hydrogen supplied to the reactor varies with space velocity and is the same for each catalyst at the same space velocity. The hydrogen supplied to the reactor is sufficient for the FTS up to a space time of about 0.07 to 0.09 h g(Fe) NL^{-1}; however, at higher space times (or reaction times) the hydrogen supplied to the reactor is lower than that consumed by the FTS. The extra hydrogen consumed by the FTS must be formed by the WGS reaction.

The same data can be plotted with respect to carbon monoxide conversion instead of reaction time (Figure 14). The hydrogen supplied to the reactor is now different for each catalyst as the carbon monoxide conversions are different at the same space velocities. Similar to Figure 13, the hydrogen supplied to the reactor is sufficient for the FTS at low carbon monoxide conversions (less than 50%). Further, at higher carbon monoxide conversions, part of the hydrogen needed by the FTS must be obtained from the WGS reaction due to the insufficient hydrogen supply to the reactor. This illustrates that a high rate of the WGS reaction is necessary to supply the extra hydrogen in order to have a high rate of the FTS for synthesis gas containing a low H_2/CO ratio.

There is an increasing need for hydrogen formed by the WGS reaction with increasing carbon monoxide conversion (Figure 14). Further, the extent of the WGS

reaction increases substantially with potassium loading (Figure 8). These two factors can explain the variation in the effect of potassium on synthesis gas conversion (or activity) with reaction time (Figure 2).

At low carbon monoxide conversions or reaction times the extent/rate of the WGS reaction is not critical. The hydrogen supplied to the reactor is more than sufficient for the FTS. At these conversion levels, the only determinant of the overall FTS activity is the FTS reaction (Equation 1). As shown in Figure 2, the overall FTS activity of the catalyst (given by the synthesis gas conversion) decreases with potassium loading. Hence, potassium apparently acts as a catalyst poison for the FTS reaction.

As the carbon monoxide conversion increases, the extent/rate of the WGS becomes increasingly critical. The overall FTS activity is increasingly dependent on the hydrogen formed by, and thus the rate of, the WGS reaction. The overall FTS activity is then determined not only by the FTS reaction (Equation 1) but also by the WGS reaction (Equation 2). The highest overall FTS activity (synthesis gas conversion) at intermediate carbon monoxide conversions should then be exhibited by a catalyst which has an acceptably high rate for both the FTS reaction (Equation 1) as well as the WGS reaction (Equation 2). Since, the extent of the WGS reaction increases with potassium loading, the overall FTS activity should be a maximum at intermediate potassium loadings at these intermediate carbon monoxide conversions levels. This is exactly the situation at intermediate carbon monoxide conversion levels (Figure 2) where the synthesis gas conversion is the highest for the catalyst with an intermediate potassium loading (1.4 K).

At high carbon monoxide conversions, the overall FTS activity is increasingly dominated by the WGS reaction rather than the FTS reaction. Hence, the overall FTS activity should be higher for catalysts having a high rate for the WGS reaction. Since the extent of the WGS reaction increases with potassium loading, this implies that the overall FTS activity should be the highest for the catalyst with the highest potassium content. As shown in Figure 2, at high carbon monoxide conversions the synthesis gas conversion is maximum for the 2.2 K catalyst.

In summary, the above reasoning provides a consistent explanation for the experimental results of varying optimum potassium loadings with space velocity (Figure 2). According to this explanation, potassium actually inhibits the rate of the FTS reaction (Equation 1). Varying optimum potassium loadings with synthesis gas conversion level are due to the enhancement of the WGS reaction by potassium.

Effect of Water Partial Pressure

The partial pressure of water or the ratio of the partial pressure of water to the product of the partial pressures of carbon monoxide and hydrogen inhibit the FTS rate according to Equation (3). A possible explanation for changes in catalyst activity with potassium loading is the corresponding change in the water partial pressure or the partial pressure ratio with potassium loading. However, a comparison of Figures 4 or 5 with Figure 1 does not show any correlation between the partial pressures and synthesis gas conversion for the three potassium loadings studied. For instance, the water partial pressure decreases with potassium loading at the same space velocity whereas the synthesis gas conversion does so only at high space velocities and does not at low and intermediate space velocities.

Effect of Potassium on Kinetic Parameters

Figures 13 and 14 clearly show that the FTS reaction must depend increasingly on the hydrogen formed by the WGS reaction as the reaction time or carbon monoxide conversion increases. Thus the overall FTS rate is increasingly affected by the rate/extent of the WGS reaction at high conversions. Only at lower conversions is the overall FTS rate unaffected by the WGS reaction. Hence, there is a change in the rate limiting step of the overall FTS reaction (Equation 1 or Equation 2) with carbon monoxide conversion. This provides an explanation for the non-linearity of the experimental results when plotted (Figure 9) according to the linearized version of Equation 3. The results at carbon monoxide conversions of less than 60% lie on a straight line; however, results at higher carbon monoxide conversions deviate substantially.

Since, the rate of the FTS reaction is of importance in this study, regression lines have been drawn in Figure 9 for the data at carbon monoxide conversions below 60%. Information obtained from these regression lines then correspond only to the FTS reaction (Equation 1) and not to any influence of the WGS reaction (Equation 2). The intercept and slope of the regression lines can be used to calculate the rate constant (k) and the adsorption parameter (b) with potassium loading.

The rate constant (k) decreases with potassium loading as shown in Figure 15. This decrease in the rate constant is more than an order of magnitude between loadings of 0.36 K and 2.2 K. This result is consistent with the explanation offered for varying optimum potassium loadings with conversion level wherein the potassium was shown to be a poison or decrease the catalyst activity for the FTS reaction (Equation 1).

The adsorption parameter (b) also decreases with potassium loading as shown in Figure 16. Similar to the extent of decrease in the rate constant, the adsorption parameter decreases by over an order of magnitude between 0.36 K and 2.2 K loadings. The adsorption parameter has been shown to be given by (5)

$$b \propto \frac{K_{H_2O}}{K_{CO}} \qquad \textbf{(11)}$$

where K_{H_2O} and K_{CO} are adsorption equilibrium constants for water and carbon monoxide respectively. Thus a decrease in the adsorption parameter (b) can be due to a decrease in the adsorption equilibrium constant for water and/or an increase in the adsorption equilibrium constant for carbon monoxide. Several previous studies (3,9,10) have shown that potassium causes an increase in the adsorption equilibrium constant for carbon monoxide. The observed decrease in the adsorption parameter (b) with potassium loading is consistent with the results of these studies.

A decrease in the rate constant (k) with potassium loadings implies a decrease in the FTS rate with potassium loading. In contrast, a decrease in the adsorption parameter (b) with potassium loading implies an increase in the FTS rate with potassium loading. This provides a possible explanation for a maximum in FTS activity with potassium loading. Thus an optimum potassium loading would be one for which the rate constant (k) is not too low and the adsorption parameter (b) not too high.

Effect of Potassium on Selectivity

As illustrated in Figure 10, increasing the amount of potassium on the catalyst appears to increase the selectivity to ethene. This is in conformity to previous studies. However, the selectivity to propene depends on the carbon monoxide conversion level.

This is in contrast to previous studies and illustrates the importance of comparing selectivities at similar carbon monoxide conversion.

Since the selectivity to 1-butene relative to total butenes increases with increasing potassium loading (Figure 11), the isomerization ability of the catalyst decreases with increasing amounts of potassium. Similarly, the selectivity to methane decreases with increasing potassium loading at carbon monoxide conversions greater than 50%.

CONCLUSION

A systematic evaluation of the effect of potassium on FTS activity and selectivity has been carried out in this study. A major observation of this study is that the trends in FTS activity with potassium loading are dependent on the space velocity and synthesis gas conversion level. At low synthesis gas conversions, the FTS activity decreases with potassium loading. At intermediate synthesis gas conversions, there is a maximum in FTS activity with potassium loading. At high synthesis gas conversions, potassium slightly enhances the FTS activity.

A consistent explanation for these activity trends has been given. The overall FTS activity is independent of the WGS reaction at low synthesis gas conversions. Potassium acts as a catalyst poison at these conversion levels as the FTS activity decreases with potassium loading. As the synthesis gas conversion increases, the hydrogen supplied to the reactor is insufficient for the FTS and the FTS increasingly depends on the hydrogen formed by the WGS reaction. Further, the extent of the WGS reaction increases with potassium loading. Thus as synthesis gas conversion increases the maximum overall FTS activity is obtained first at intermediate potassium loadings and finally at the highest potassium loading used in this study.

The effect of potassium on kinetic parameters for the FTS has also been determined in this study. The FTS activity depends on a rate constant and an adsorption parameter according to a previously proposed rate expression (5). The rate constant decreases by more than an order of magnitude when the potassium loading is increased from 0.36 K to 2.2 K. Thus potassium acts as a catalyst poison for the FTS. The adsorption parameter also decreases by over an order of magnitude with increasing potassium loadings between 0.36 K and 2.2 K. Since decreases in the rate constant and the adsorption parameter affect the FTS rate in opposite directions, these results provide a reasonable explanation for a maximum in FTS activity with potassium loading. Hence, an optimum potassium loading is one for which the rate constant is not too low and the adsorption parameter not too high.

Unlike previous studies, the effect of potassium on catalyst selectivity has been compared at similar conversions. The effect of increasing amounts of potassium on alkene selectivity depends on the number of carbon atoms of the hydrocarbons as well as the carbon monoxide conversion level. The extent of isomerization decreases with potassium loading. The selectivity to methane in the total hydrocarbon product is affected by potassium at carbon monoxide conversions above 50% and increases with decreasing potassium loading.

ACKNOWLEDGMENT

This work was supported by U.S. DOE contract number DE-AC22-94PC94055 and the Commonwealth of Kentucky.

REFERENCES

1. Anderson, R. B., Seligman, B., Shultz, J. F., Kelly, R. and Elliott, M. A., *Ind. Eng. Chem.*, **44**, 391 (1952).
2. Dry, M. E., in **?***Catalysis-Science and Technology"*, (J.R. Anderson and M. Boudart, eds.), Springer, Berlin (1981).
3. Arakawa, H. and Bell, A. T., *Ind. Eng. Chem. Proc. Des. Dev.*, **22**, 97 (1983).
4. Bukur, D. B., Mukesh, D. and Patel, S. A., *Ind. Eng. Chem. Res.*, **29**, 194 (1990).
5. Huff, G. A. and Satterfield, C. N., *Ind. Eng. Chem. Proc. Des. Dev.*, **23**, 696 (1984).
6. Raje, A. P. and Davis, B. H., *Catalysis Today*, **36** (1997) 335.
7. Davis, B. H., Tau, L. M., Dabbagh, H. and Chawla, B., Mechanism of Promotion of Fischer-Tropsch Catalysts", DOE/PC/70029-T1, Final Report, December 1987.
8. Xu, L., Bao, S., O'Brien, R. J., Houpt, D. J. and Davis, B. H., *Fuel Sci. Tech. Int.*, **12**, 1323 (1994).
9. Dry, M. E., Shingles, T., Boshoff, L. and Oosthuizen, G. J., *J. Catal*., **15**, 190 (1969).
10. Benziger, J. and Madix, R., *Surf. Sci.*, **94**, 119 (1980).

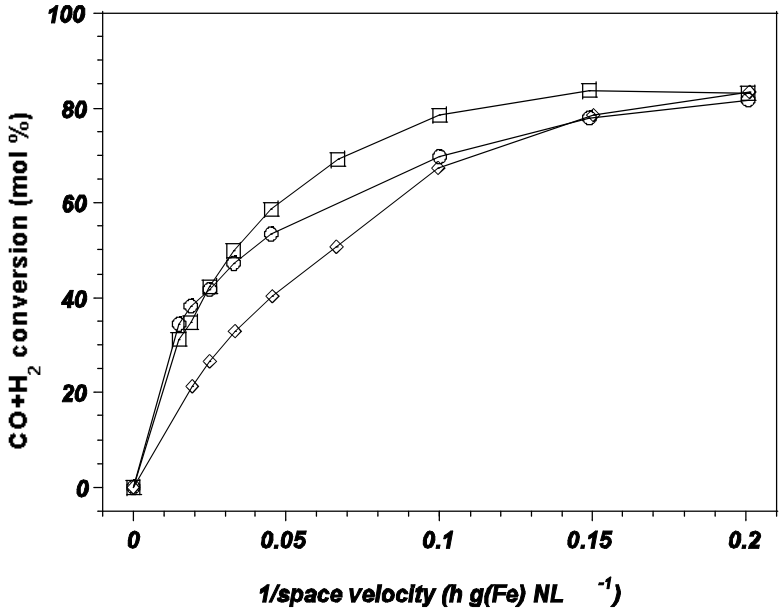

Figure 1. Synthesis gas conversion as a function of potassium loading. (**F**) 0.36 K, (**G**) 1.4 K, and (•) 2.2 K.

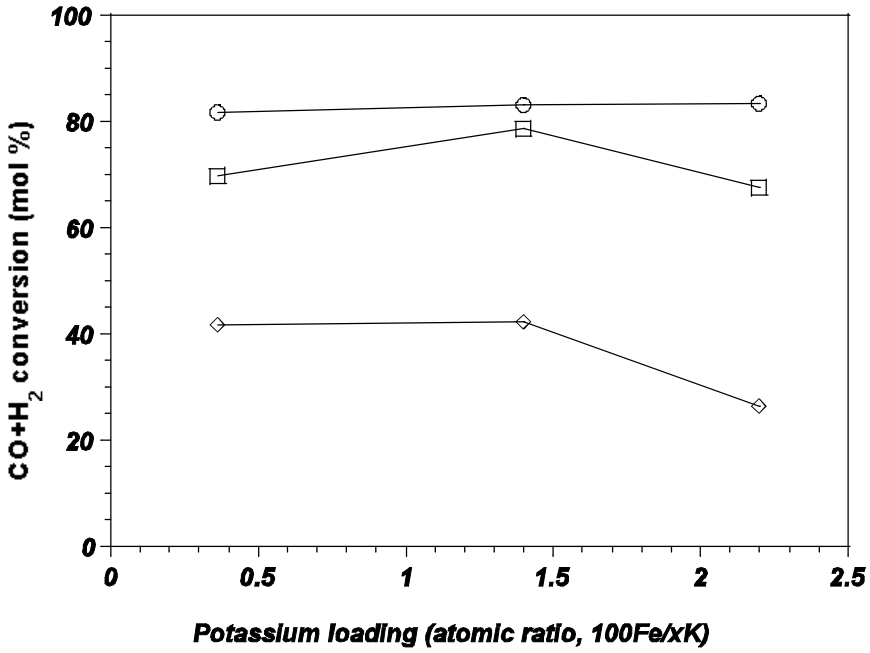

Figure 2. Synthesis gas conversion as a function of potassium loading. (**F**) 5 NL h^{-1} $g(Fe)^{-1}$, (**G**) 10 NL h^{-1} $g(Fe)^{-1}$ and (•) 50 NL h^{-1} $g(Fe)^{-1}$.

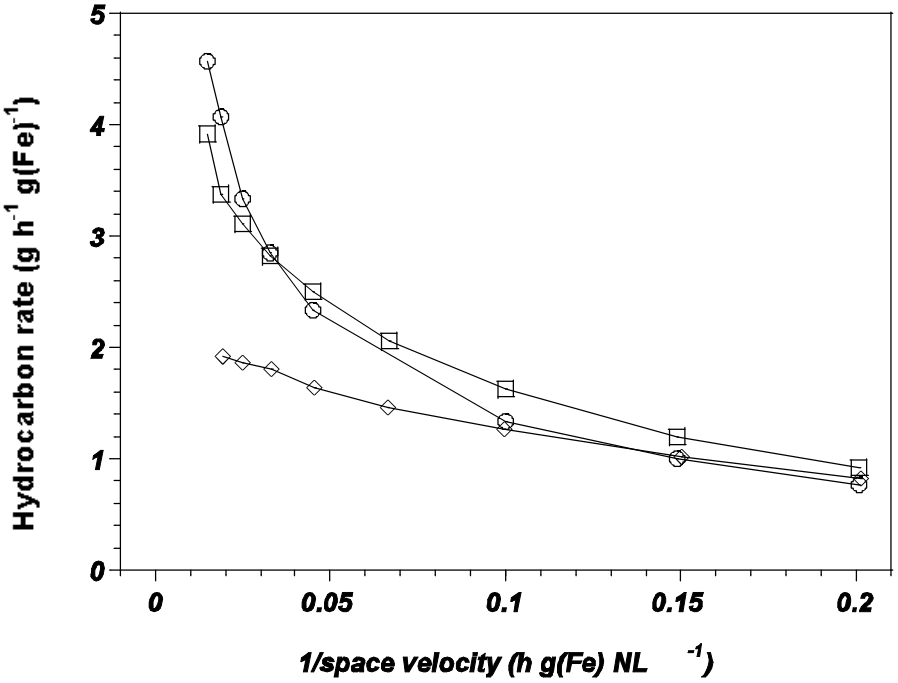

Figure 3. Hydrocarbon production rate as a function of reciprocal flow rate. (**F**) 0.36 K, (**G**) 1.4 K, and (•) 2.2 K.

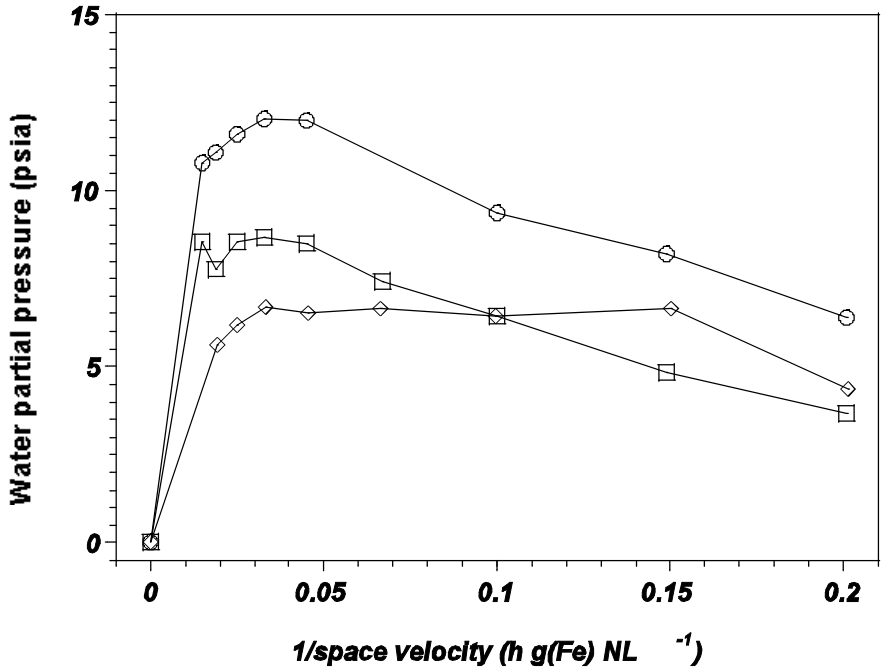

Figure 4. Water partial pressure as a function of reciprocal flow rate. (**F**) 0.36 K, (**G**) 1.4 K, and (•) 2.2 K.

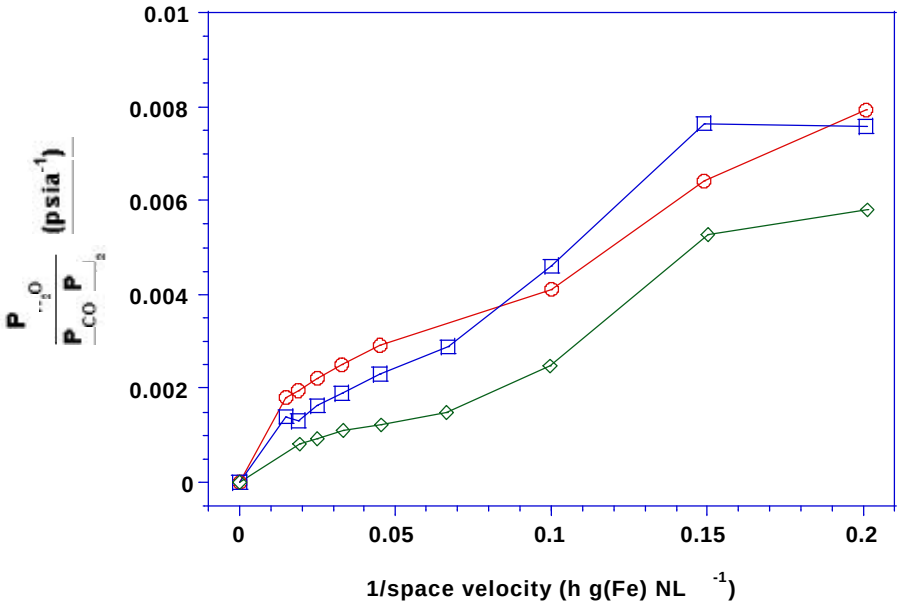

Figure 5. Partial pressure ratio, $\frac{P_{H_2O}}{P_{CO}P_{H_2}}$ as a function of reciprocal flow rate. (**F**) 0.36 K, (**G**) 1.4 K, and (•) 2.2 K.

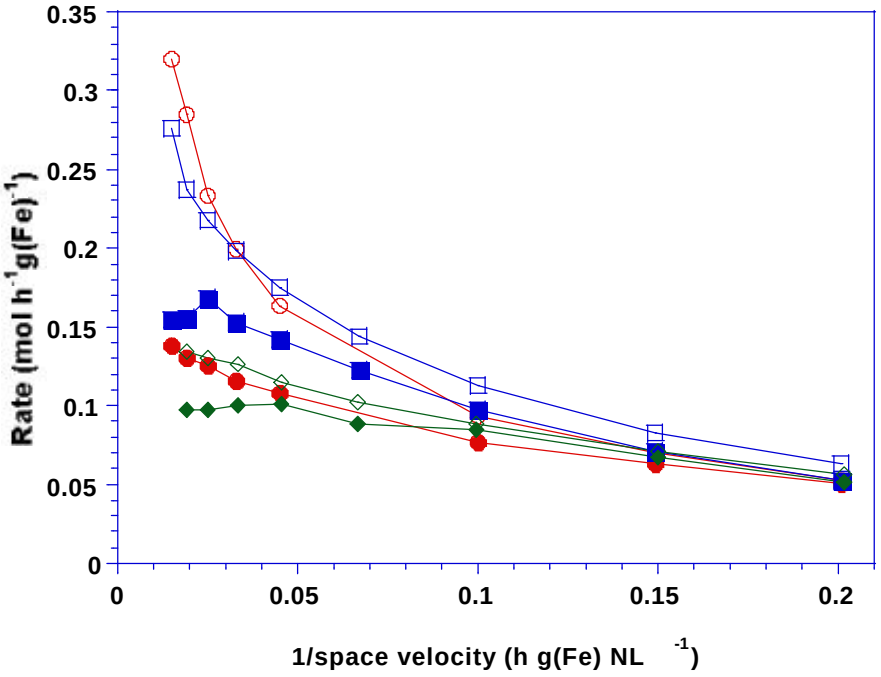

Figure 6. Fischer-Tropsch (open symbols) and water-gas shift (closed symbols) rates as a function of reciprocal flow rate. (**F**) FT; 0.36 K, (**M**) WGS; 0.36 K, (**G**) FT; 1.4 K, (**O**) WGS; 1.4 K, (**"**) FT; 2.2 K, and (**–**) WGS; 2.2 K.

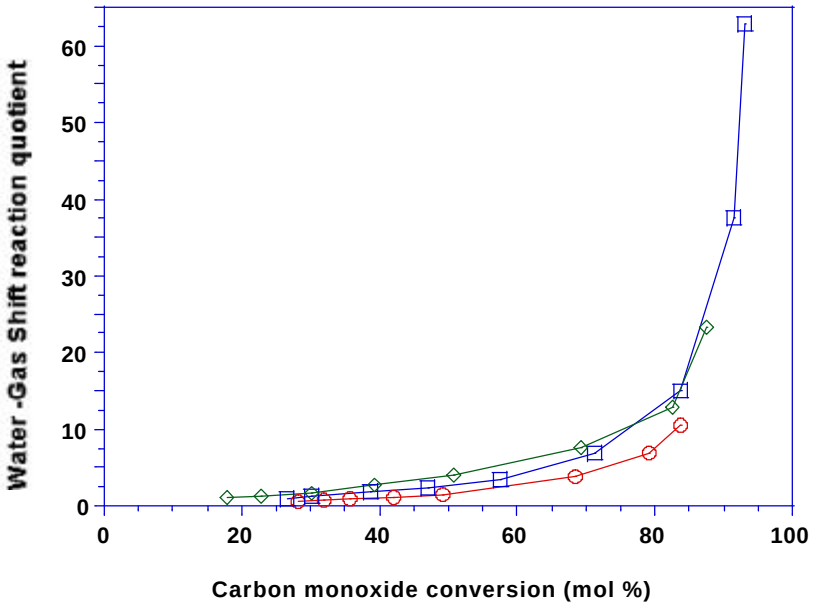

Figure 7. Water-gas shift reaction quotient as a function of reciprocal flow rate. (**F**) 0.36 K, (**G**) 1.4 K, and (•) 2.2 K.

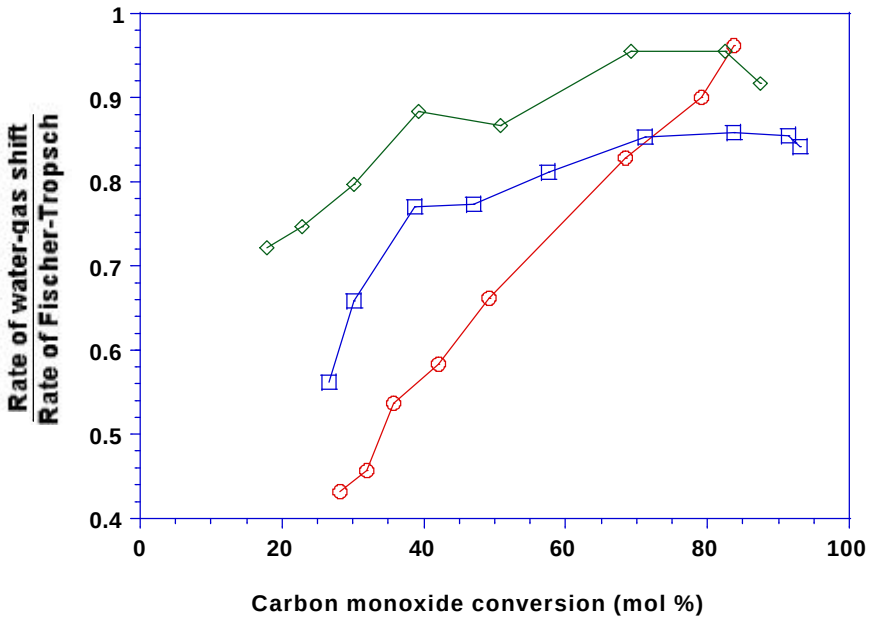

Figure 8. Ratio of rate of Fischer-Tropsch synthesis to rate of water-gas shift reaction as a function of reciprocal flow rate. (**F**) 0.36 K, (**G**) 1.4 K, and (•) 2.2 K.

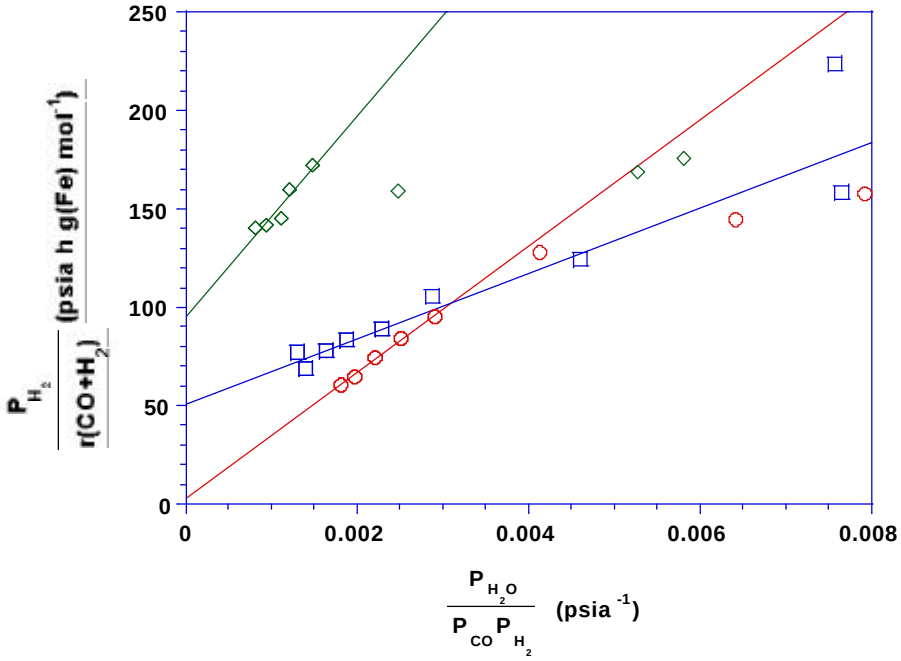

Figure 9. Plots of the linearized version of equation 3. (**F**) 0.36 K, (**G**) 1.4 K, and (•) 2.2 K.

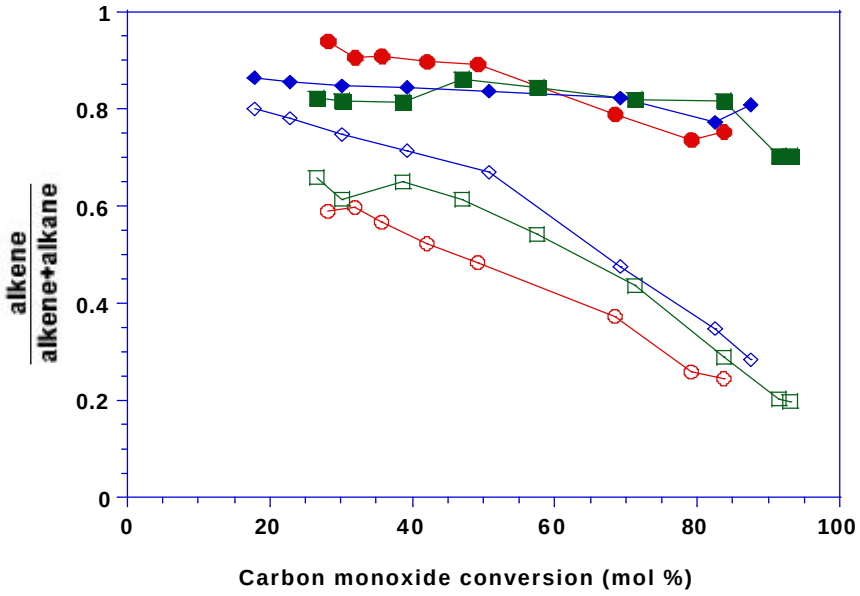

Figure 10. Alkene selectivity of C_2 (open symbols) and C_3 (closed symbols) hydrocarbons. (**F**) C_2; 0.36 K, (**M**) C_3; 0.36 K, (**G**) C_2; 1.4 K, (**O**) C_3; 1.4 K, (•) C_2; 2.2 K, and (**–**) C_3; 2.2 K.

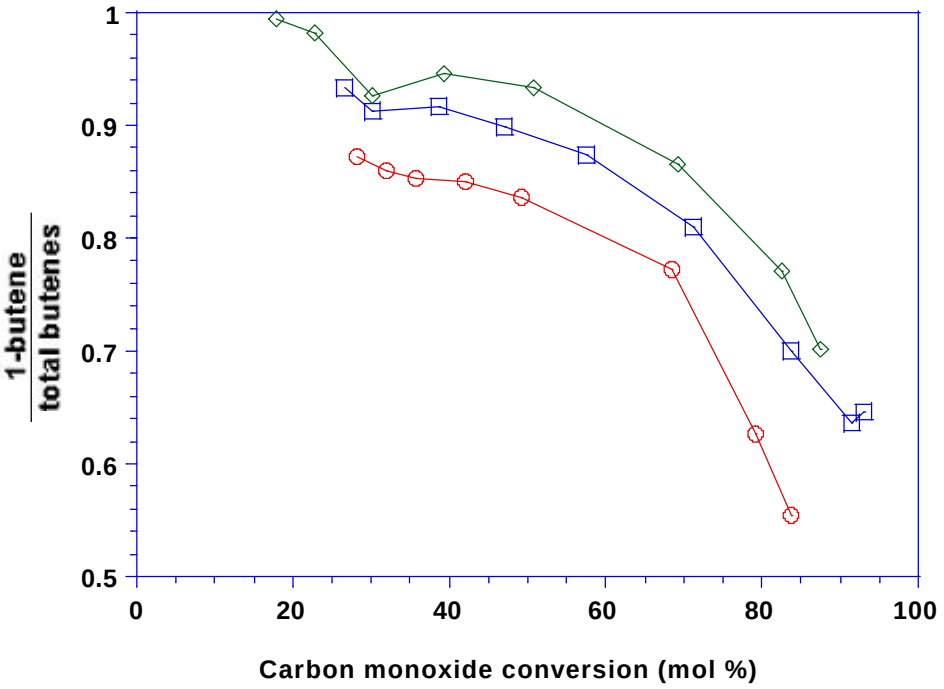

Figure 11. Fraction of 1-butene in total linear alkenes as a function of carbon monoxide conversion. (**F**) 0.36 K, (**G**) 1.4 K, and (•) 2.2 K.

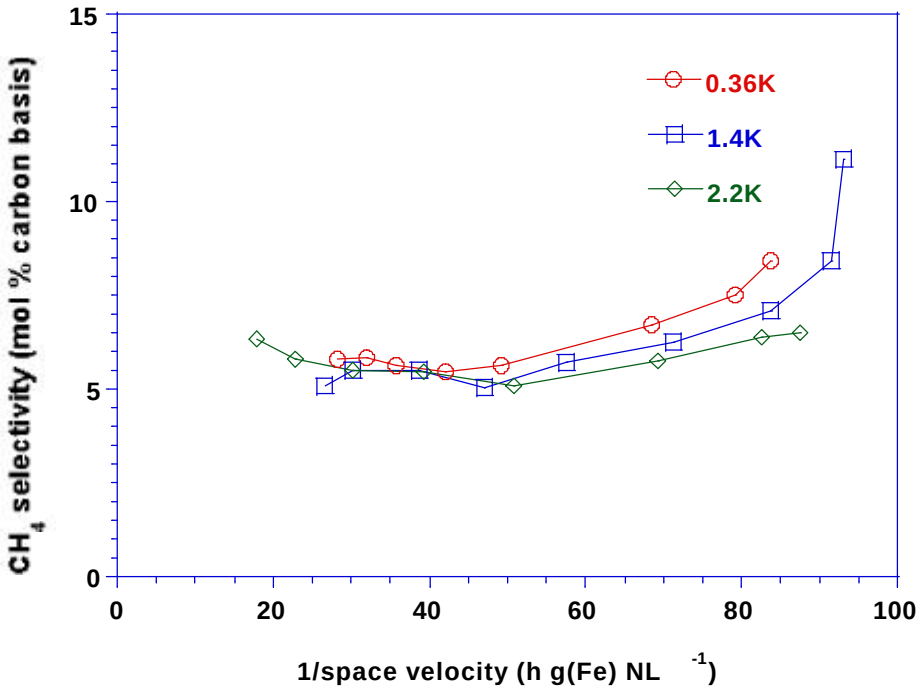

Figure 12. Methane selectivity as a function of carbon monoxide conversion. (**F**) 0.36 K, (**G**) 1.4 K, and (•) 2.2 K.

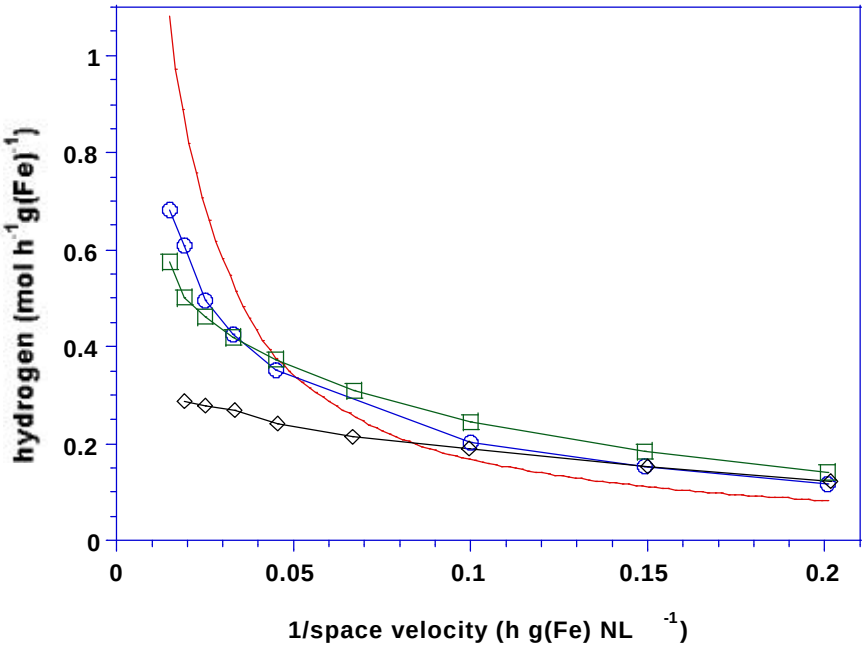

Figure 13. Need for water-gas shift reaction shown as a comparison of hydrogen supplied to the reactor and hydrogen used by the FTS. (—) hydrogen supplied to reactor, (**F**) hydrogen used by 0.36 K catalyst, (**G**) hydrogen used by 1.4 K catalysts, and (•) hydrogen used by 2.2 K catalyst.

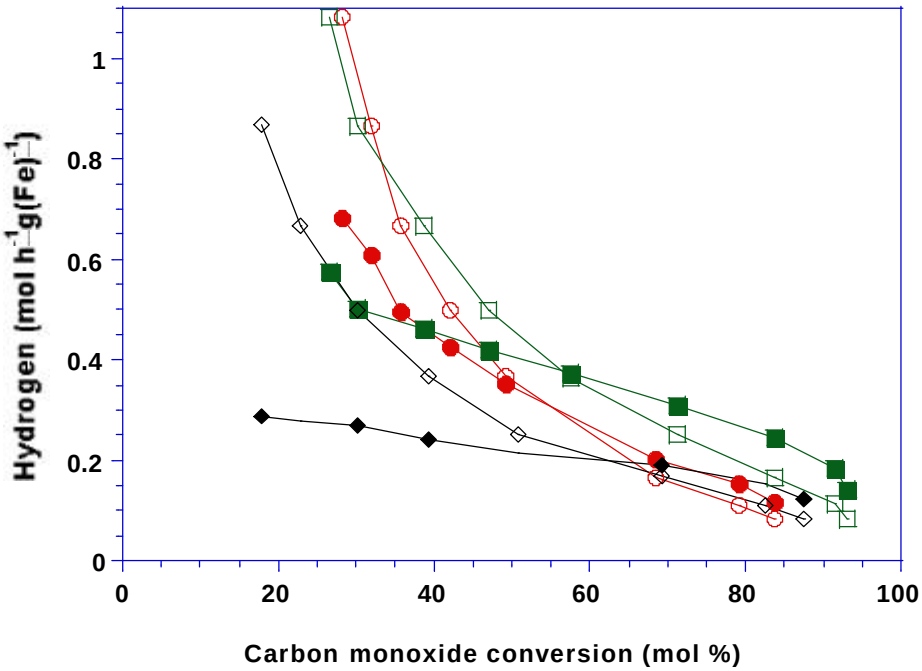

Figure 14. Need for water-gas shift reaction with increasing carbon monoxide conversion. Open symbols: hydrogen supplied to reactor. Closed symbols: hydrogen used by FTS. (**F**, **M**) 0.36 K, (**G**, **O**) 1.4 K, and (**",–**) 2.2 K.

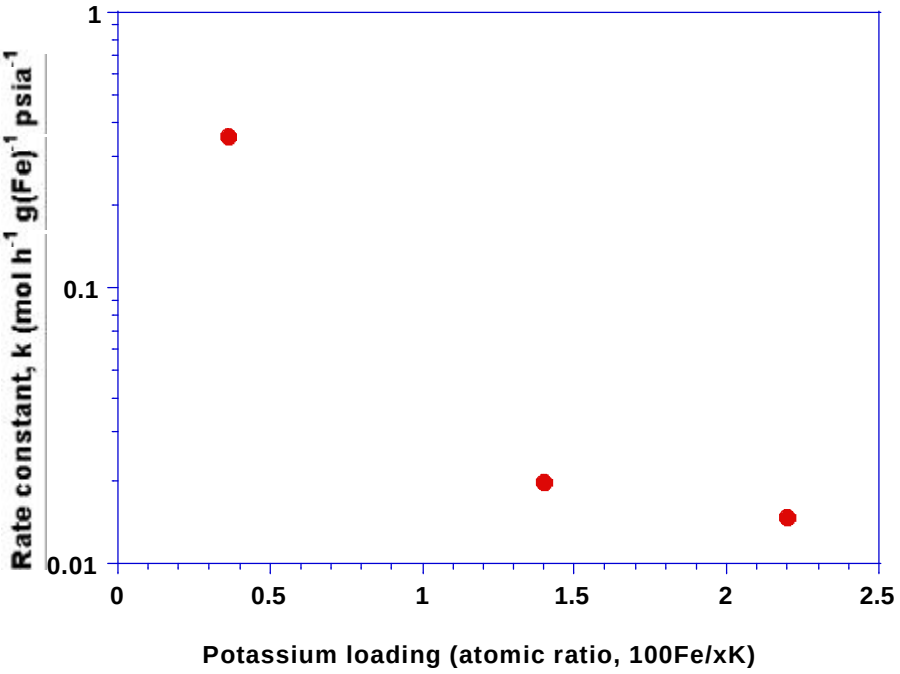

Figure 15. Fischer-Tropsch rate constant as a function of potassium loading.

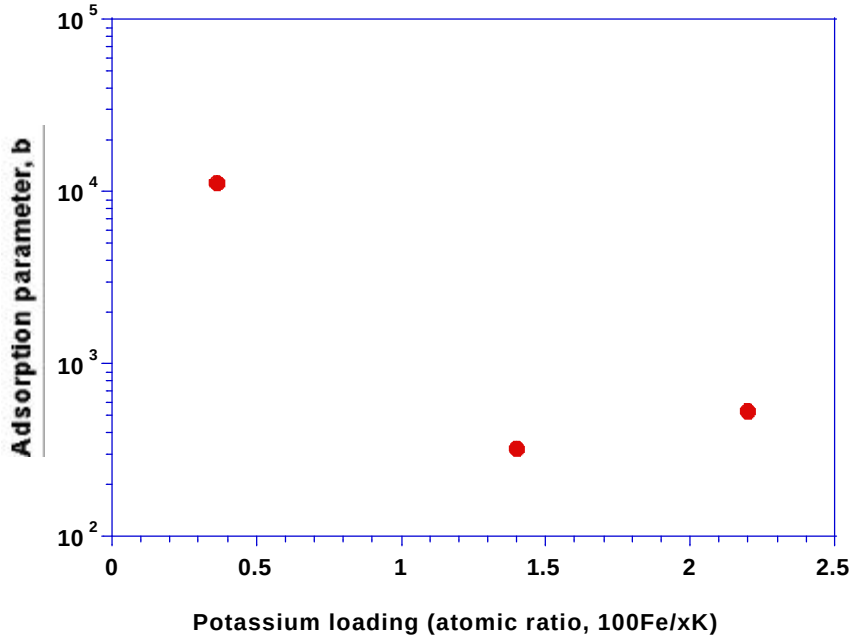

Figure 16. Adsorption parameter (b) from equation 3 as a function of potassium loading.

3.1.3 Fischer-Tropsch Synthesis. Compositional Changes in an Iron Catalyst During Activation And Use

ABSTRACT

The equilibrium phase compositions of iron have been calculated for gas compositions that could be encountered during the Fischer-Tropsch synthesis. The gas compositions measured experimentally for CO conversion levels in the 30-90% range show that iron should be present as the carbide phase. However, experimental characterization of iron catalysts show that a significant fraction of the iron is present as Fe_3O_4 following synthesis for several days. A model that can account for the experimental catalyst phase composition and the gases present in the reactor would have a core of Fe_3O_4 and an outer layer of iron carbides.

INTRODUCTION

The CHO system is of great importance in many areas of modern technology, including combustion, gasification, fuel cell and the Fischer-Tropsch (F-T) synthesis process. The species most likely to be present in the greatest amounts are those which are most stable under the conditions of interest, i.e., those having the lowest values of the free energy of formation. For the system containing carbon, hydrogen and oxygen in the temperature ranges of 298K to 1500K and a pressure of one atmosphere, the most stable species are carbon, carbon oxide, carbon dioxide, hydrogen, water and methane (1). For the F-T synthesis reaction, an iron catalyst is frequently employed. On contacting with the pretreating and/or synthesis gases, the iron or iron oxides can form an iron carbide, which is a catalyst for F-T synthesis. It is

of interest to define the gas phase compositions where the iron carbide is thermodynamically favored during the course of catalyst activation and synthesis.

A convenient and informative method for the presentation of the iron carbide or iron oxide formation boundaries for the ternary CHO system is a set of triangular coordinates. The generality of the phase diagram becomes clear when it is recognized that C:H:O ratios of the system completely determine whether or not carbon, iron oxide and/or iron carbide will form for a given composition of gases. The usefulness of the phase diagram has been demonstrated by Manning and Reid (2) in their study of the iron-iron oxide system, Sacco and Reid (3) for the Bosch reaction system, and Sacco et al. (4) who studied the formation of carbon on iron.

This study considers the CHO gas phase compositions in equilibrium with iron and/or graphite (C) over the temperature range of interest for Fischer-Tropsch synthesis (200^{o}C - 300^{o}C) at pressures of 1 and 15 atmospheres. Different forms of iron oxide, i.e., Fe_3O_4, Fe_2O_3 and FeO, and iron carbide, i.e., Fe_3C, $Fe_{2.2}C$ and Fe_2C, may be present during F-T synthesis. However, for simplicity and the availability of thermodynamic data, only Fe_3O_4 and Fe_3C are used to represent the iron compounds in these calculations.

In the F-T synthesis using an iron catalyst, Fe_3C, Fe_3O_4, and C may form by reactions (1), (2) and (3), respectively:

$$H_2 + CO + 3Fe \rightleftharpoons Fe_3C + H_2O \quad (1)$$

$$3Fe + 4H_2O \rightleftharpoons Fe_3O_4 + 4H_2 \quad (2)$$

$$2CO \rightleftharpoons C + CO_2 \quad (3)$$

The gas components are also subject to water-gas shift reaction:

$$H_2O + CO \rightleftharpoons H_2 + CO_2 \quad (4)$$

and methane is included as follows:

$$C + 2H_2 \rightleftharpoons CH_4 \quad (5)$$

Also, hydrocarbons may be formed as, for example:

$$CO + H_2 \rightleftharpoons CH_2 + H_2O \quad (6)$$

$$nCH_2 \rightleftharpoons (CH_2)_n \quad (7)$$

RESULTS

Three pertinent equilibria, C/gases, Fe/Fe_3O_4/gases and Fe/Fe_3C/gases were considered in the calculations. A modification of the method presented by Cairns and Tevebaugh was employed (1). Details of the calculation are given in Appendix A. Figures 1 to 3 are phase diagrams showing the Fe/Fe_3O_4/gases (**9**), Fe/Fe_3C/gases (ª) and C/gases (**"**) at 15 atm. total pressure and temperatures of 300, 200 and 270°C, respectively. These graphs are on a molar basis of C, O and H; thus, an equimolar mixture of H, C and O (0.33 moles of each) requires a syngas with $H_2/CO = 0.5$. From these diagrams, one can delineate regions where Fe_3C, Fe_3O_4 and/or C would be expected to form when iron is in contact with different gas mixtures composed of hydrogen, oxygen and carbon at different temperatures. For example, for a gas mixture represented by a position which is located above the upper line (**G**), Fe_3C is the solid iron phase that is thermodynamically favored. Carbon could also be formed in this region if Fe_3C catalyzed carbon formation at a rate comparable to F-T; i.e., reaction (3) would proceed to the right. The tie line for syngas of different H_2/CO mole ratios is also included in Figure 1. This tie line clearly shows that in order to have iron present only as Fe_3C, the H_2/CO mole ratio of the syngas must be less than about 0.75 at 300°C.

After activation with CO, the iron should be present only as a carbide. Experimental data show the 90% or greater is present as iron carbide following a 24 hr

activation period (5-7). During the course of F-T synthesis gas compositions change to produce a catalyst in which some Fe_3C is converted to Fe_3O_4 (Figure 4, from ref. 5). Previous studies produced data to show that the formation of H_2O during the F-T synthesis, i.e., reaction 6, is a major reason that Fe_3C will change phase to Fe_3O_4 (8). For a particular feedstock that defines the ratio of H_2/CO, the composition of all gases can be calculated by using material balance equations for each conversion level of CO and H_2.

The minimum time required for the catalyst phase change can be established. Assume that pure Fe_3C is placed in a "flexible reactor" whose volume can increase or decrease but maintain a constant pressure, i.e. 15 atm. The feed gas is continuously charged into this reactor at a constant flow rate. Gases may react with Fe_3C to covert it to Fe_3O_4 until the equilibrium composition is established. This equilibrium reaction can be described as (8) and/or (9):

$$Fe_3C + 4H_2O = Fe_3O_4 + 2H_2 + CH_4 \quad (8)$$

or

$$Fe_3C + 5CO_2 = Fe_3O_4 + 6CO \quad (9)$$

Using these equations one can calculate the time needed to convert Fe_3C to Fe_3O_4 at a particular reaction condition. For our typical F-T synthesis conditions (catalyst = 15 g of Fe, T = 270^{o}C, P = 15 atm, H_2/CO = 0.67 at a flow rate of 3.1 NL/hr./g of Fe, and alpha value is 0.7), the H_2 and CO conversions are approximately 0.9 and 0.86, respectively (9,10). Under this reaction condition, the percentage change of Fe_3C to Fe_3O_4 with time and total amount of gases in the flexible reactor can be calculated. It takes approximately 4 hours to have sufficient gas flow to convert Fe_3C to the

equilibrium composition of Fe_3O_4 and Fe_3C. The volume of syngas needed to convert Fe_3C to a mixture with the equilibrium amount of Fe_3O_4 is approximately 15 liters (at 15 atm and 300^{o}C; 120 NL at 1 atm and 25^{o}C). The actual time for this conversion is actually much longer than this (e.g., Figure 4).

Comparison with Experimental Data

F-T synthesis was effected at various CO conversion levels using a slurry reactor. Details of the experimental set-up, procedures and analytical methods are provided elsewhere (9,10). The molar ratio of syngas feed (H_2/CO=0.67), pressure (175 psi), and temperature (270^{o}C) were held constant while flow rates of syngas were varied between 9.5 and 75.6 NL/hr-gFe for CO (6.4 and 50.6 NL/hr for H_2). The composition of the gas phase exiting the reactor for each conversion level is shown in Table 1. The hydrocarbons formed (i.e., C_1 to C_{35}) during the reaction are reported in this table as an average value of $C_x H_y$. The mean carbon number of the hydrocarbon products is given by equation 10 (10):

$$x = 1/ (1 - a) \qquad (10)$$

where a refers to chain growth probability. Since the a value for these particular run is about 0.75 (8,9), the mean carbon number, x, is 4. The mean hydrogen number in the products can be calculated by:

$$y = \{ \sum [H/C]_i \bullet N_i / \sum N_i \} * x \qquad (11)$$

where the mean carbon number x = 4, i denotes hydrocarbon with carbon number equal to i, and N denote the molar fraction of each hydrocarbon. The data in Figure 5 indicate that at higher conversion levels, (X_{CO} = 0.69 to 0.86), Fe_3C is the solid iron phase that is favored by thermodynamics. However, at lower conversion levels (X_{CO} =

0.23 to 0.46) both Fe_3C and Fe_3O_4 are thermodynamically favored. The data in Table 1 show that the concentration of H_2O increases to a maximum level and then decreases with increasing CO conversion. On the other hand, the concentration of CO_2 increases with increasing CO conversion.

The data in Figure 6 indicate that the conversion of CO and H_2 are approximately equal (i.e., $X_{CO} = X_{H_2} = 0.69$) at a total flow rate ($CO+H_2$) of 31.3 NL/hr-gFe; this equal conversion is designated the equivalence point. At flow rates lower than the one that corresponds to the equivalence point, the conversion of H_2 is greater than that of CO while the conversion of CO is greater than that of H_2 above the equivalence point. This is due to the effect of WGS reaction since it consumes CO to generate H_2. For flow rates slower than the one corresponding to about the equivalence point, Fe_3C is the iron phase that is thermodynamically favored. However, for flow rates faster than the one corresponding to the equivalence point, both Fe_3C and Fe_3O_4 are thermodynamically favored.

The solubility of the F-T gaseous reaction products, CO_2 and H_2O, in the F-T reactor wax product is reported to be higher than CO and H_2 by about a factor of ten; however, the solubilities of CO and H_2 increase remarkably with temperature which is in contrast to the product gases where the solubilities decrease with increases of temperature (12). Knowing the partial pressure of gas phase compounds and assuming that vapor-liquid equilibrium occurs, the solubility of each gas can be calculated using the data reported in references 9 and 12. The total amounts of the compounds (CO, H_2O, CO_2, CH_4) present in the reactor in both the gas and liquid phases can be calculated; these are shown in Figure 7. The data which represent both

gas and liquid phase compounds are similar to the results in Figure 5, which represent only gas phase compounds.

DISCUSSION

The thermodynamic data indicate that activation in CO or H_2/CO at compositions with a ratio of 0.7 or lower should produce a nearly pure iron carbide phase. The experimental data generated during a 24 hour activation in CO at 270^{o}C (1 or 12 atm.) show nearly pure iron carbide is formed (Figure 8). However, during about 24 hours of CO activation in a CSTR at 270^{o}C, about twice as much carbon is deposited as is required to produce an iron carbide. Thus, it is apparent that a form of free carbon is deposited as well during the 24 hour activation. It is a common feature to observe a carbon film on nanometer sized metal particles (13,14). Carbon films have also been observed an large-particle iron Fischer-Tropsch catalysis (15).

The reduction of the catalyst to iron is not expected in a static system at temperatures of 300^{o}C and lower. In agreement with this expectation, only about 30% of the iron is present as Fe^o following 24 hour at 270^{o}C in **flowing** hydrogen which continuously removes water (e.g., 5). Under reaction conditions, even at high conversion levels to produce high H_2/CO ratios, the presence of significant water (and CO_2) will prohibit the reduction of the iron to Fe^o.

Under conditions of synthesis with H_2/CO = 0.7, the calculated data based on the exit gas phase composition, and even including the excess CO and H_2O held in the liquid phase in the reactor, based upon measured solubilities, the iron catalyst should be present as the carbide phase (Figure 7). One of the reasons for the deviation of the experimental data from the equimolar C and O tie-line is that oxygen present in

methanol, ethanol and other oxygenates have not been included in the calculation. However, a significant fraction of the iron in the catalyst is present as Fe_3O_4 following long-term use in Fischer-Tropsch synthesis (16-20).

One possibility to account for the presence of both iron carbides and Fe_3O_4 during Fischer-Tropsch synthesis is that the error in the thermodynamic data causes the actual region for the presence of both iron carbides and Fe_2O_3 to extend to a higher carbon region than shown in Figures 1-3, 5 and 7.

A more likely possibility is inhomogeneity in the individual catalyst particles. In the interior of the individual porous particle and in the agglomeration of particles, the conversion of H_2 and CO to produce CO_2 and H_2O in addition to liquid hydrocarbons can serve to increase the concentration of H_2O and CO_2 to levels that are higher than are present in the bulk gas phase. Thus, the individual catalyst particles could be present with a core of predominantly Fe_3O_4 and with a surface layer of predominantly iron carbides coating the Fe_3O_4 core.

Various studies at the CAER have shown that a sample activated to produce a material that is predominantly Fe_3O_4 has a much lower catalytic activity than one that is predominantly an iron carbide. Furthermore, the phases present are in a dynamic situation that depends upon the conversion levels of CO and H_2. Thus, at the surface of the catalyst particle, the CO appears to serve to imitate and to grow the hydrocarbon chains as well to serve as a source of carbon to maintain at least the surface region of the catalyst particle as an iron carbide phase.

REFERENCES

1. E. J. Cairns and A. D. Tevebaugh, J. of Chemical and Engineering Data, **9**, No. 3, 453 (1964).
2. M. P. Manning and R. C. Reid, Ind. Eng. Chem. Process Design Develop., **16**, No. 3, 358 (1977).
3. A. Sacco, Jr., and R. C. Reid, AICHE J., **25**, No. 5, 839 (1979).
4. A. Sacco, Jr., P. Thacker, T. H. Chang, and A. T. S. Chiang, J. of Catalysis, **85**, 224 (1984).
5. C. S. Huang, B. G. Ganguly, G. P. Huffman, F. E. Huggins and B. H. Davis, *Fuel Sci. Tech. Int.,* **11**, 1289 (1993).
6. K. R. P. M. Rao, F. E. Huggins, V. Majahan, G. P. Huffman, V. U. S. Rao, B. L. Bhatt, D. B. Bukur, R. J. O'Brien and B. H. Davis, *Topics in Catal.*, **2**, 71 (1995).
7. K. R. P. Rao, F. E. Huggins, G. P. Huffman, R. J. Gormley, R. J. O'Brien and B. H. Davis, *Energy & Fuels*, **10**, 546 (1996).
8. J. A. Amelse, L. H. Schwartz and J. B. Butt, *J. Catal.,* **72**, 95 (1981).
9. A. Raje, J. Inga and B. H. Davis, *Fuel*, **76**, 273 (1997).
10. A. Raje and B. H. Davis, *Catal. Today*, **36**, 335 (1997).
11. L. Caldwell and D. S. Van Vuuren, *Chem. Eng. Sci.*, **41**, 89 (1986).
12. H. Kölbel, P. Ackermann and Fr. Engelhardt, *Erdöl und Kohl*, **9**, 153 (1956).
13. P. E. Nolan, D. C. Lynch and A. H. Cutler, *Carbon*, **32**, 477 (1994).
14. R. Ochoa, X. X. Bi, A. M. Rao and P. C. Eklund in "Transition Metal Nitride and Carbide Nanoparticles," Blackie, Glasgow, United Kingdom, 1996, pp 489-510.

15. A. K. Datye, M. D. Shroff, M. S. Harrington, A. G. Sault and N. B. Jackson, "Natural Gas Conversion IV," (M. dePontes, et al., eds.) Elsevier, Amsterdam, 1997, pp 169-174.

16. B. H. Davis, *Appl. Catal. A*, **119**, 205 (1994).

17. R. J. O'Brien, L. Xu, D. R. Milburn, Y.-X. Li, K. J. Klabunde and B. H. Davis, *Topics in Catal.*, **2**, 1 (1995).

18. K.R.P.M. Rao, F. E. Huggins, V. Mahajan, G. P. Huffman, , V.U.S. Rao, B. L. Bhatt, D. B. Bukur, R. J. O'Brien and B. H. Davis, *Topics in Catal.*, **2**, 71 (1995).

19. R. J. O'Brien, L. Xu, X. X. Bi, P. C. Eklund and B. H. Davis, Fischer-Tropsch synthesis and XRD characterization of an iron carbide catalyst synthesized by laser pyrolysis, in "The Chemistry of Transition Metal Carbides and Nitrides," (S. T. Oyama, Ed.), Chapman & Hall, London, pp 362-372, 1996.

20. K. R. P. M. Rao, F. E. Huggins, G. P. Huffman, R. J. Gormley, R. J. O'Brien and B. H. Davis, *Energy & Fuels*, **10**, 546 (1996).

Appendix 1

Method for Calculation

For a balanced chemical process, the change in thermodynamic property can be calculated by adding together the tabulated values of the property for the substances present in the final state minus the sum of the values of the properties for the substances in the initial state, each value being property multiplied by the appropriate stoichiometric coefficient. The procedures for calculating the equilibrium constant for a chemical reaction utilized obtains thermodynamic properties from reference (1). The equilibrium constants for each temperature were calculated from Gibbs free energy, obtained for the $?H^o$ and $?S^o$ fractions using the assumption of $?C_p^o$ is constant in the temperature range utilized.

Equilibrium Calculation for Different Systems

The calculation for the system of C (graphite) and gases (CO, H_2, CO_2, H_2O, CH_4) equilibria, equations (3), (4) and (5) can be utilized. One material balance equation and three equilibrium constants collectively include all six species in equations (3), (4) and (5).

Material Balance		
Species	Moles at Start	Moles at Equilibrium
CO_2	$CO_{2,0}$	$CO_{2,0} - x + y$
H_2	$H_{2,0}$	$H_{2,0} - x - 2z$
C	0	y - z
CH_4	0	z
H_2O	0	x
CO	0	x - y

The variable x, y, and z can be calculated by substituting expressions from material balance into the equilibrium constant equations:

$$\frac{z}{(H_{2,0} \& x \& 2z)^2} \text{ ' } K_3 \qquad \textbf{(11)}$$

$$\frac{(CO_{2,0} \& x \% y)}{(x \& 2y)^2} \text{ ' } K_2 \qquad \textbf{(12)}$$

$$\frac{?Q(x \& 2y)}{(CO_{2,0} \& x \% y)\ (H_{2,0} \& x \& 2z)} \text{ ' } K_1 \qquad \textbf{(13)}$$

with three equations and three variables, values for x, y and z can be obtained.

For the equilibria involving Fe_3O_4/Fe and gases (CO, H_2, CO_2, H_2O, CH_4) equation (4) and the following equations are applicable:

$$2CO + 2H_2 = CO_2 + CH_4 \qquad (14)$$

$$3Fe + 4CO_2 = Fe_3O_4 + 4CO \qquad (15)$$

The appropriate compositions and equations are:

Material Balance		
Species	Initial	At Equilibrium
CO_2	0	x-y - 4z
H_2	$H_{2,0}$	$H_{2,0}$ = 2x - y
CO	$CO_{,0}$	$CO_{,0}$ - 2x + y + 4z
Fe	$Fe_{,0}$	$Fe_{,0}$ - 3z
H_2O	0	y
CH_4	0	x
Fe_3O_4	0	z

$$K_1 \text{ ' } \frac{[y]\ [CO_{,0} \& 2x \% y \% 4z]}{[H_{2,0} \& 2x \& y]\ [x \& y \& 4z]} \qquad \textbf{(21)}$$

The above allows one to obtain values for x, $[CO_2]$ and $[CH_4]$.

$$K_{2,3} \;=\; \frac{[x]\;[x\&y\&4z]}{[H_{2,0}\;\&\;2x\&y]^2\;[CO,_0\;\&\;2x\%y\%4z]^2} \qquad \textbf{(22)}$$

$$k_4 \;=\; \frac{[CO,_0\;\&\;2x\%y\%4z]^4}{[x\&y\&4z]^4} \qquad \textbf{(23)}$$

Table 1

Composition of the Gas Phase Exiting the Reactor for Each Conversion Level

Data #	H_2 (psi)	CO (psi)	H_2O (psi)	CO_2 (psi)	C_4H_y (psi)	y	X,CO (%)	X,H_2 (%)	CO+H_2 (NL/hr)
1	25.4	26.7	4	78	55	8.63	0.86	0.8	15.9
2	32	43	6	72	36	8.52	0.78	0.76	21
3	39.4	60.1	8.49	61.1	20.154	8.48	0.685	0.692	31.3
4	50.3	89.5	10.7	32.6	5.27	8.44	0.46	0.54	63.1
5	54.8	102.4	10.3	18.8	3.14	8.43	0.32	0.45	91.6
6	59.24	107.3	9.23	11.8	1.82	8.36	0.23	0.37	126.2

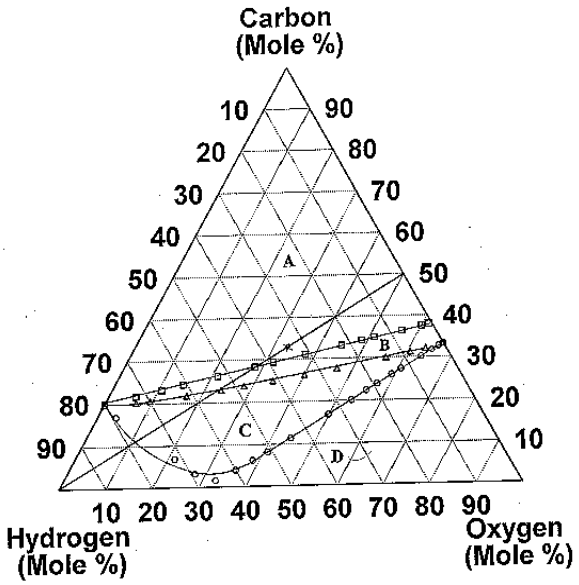

Figure 1. Ternary phase diagram for the solid phase(s) present for graphite/gases (**"**), Fe/Fe_3O_4/gases (**G**) and Fe/Fe_3C/gases mixtures at equilibrium at 300°C and 15 atm. (Region A: Fe_3C and C; Region B: Fe_3O_4, Fe_3C and C; Region C: Fe_3O_4 and C; Region D: Fe_3O_4; "—": tie line) (gases = H_2O, CO, CO_2, H_2 and CH_4).

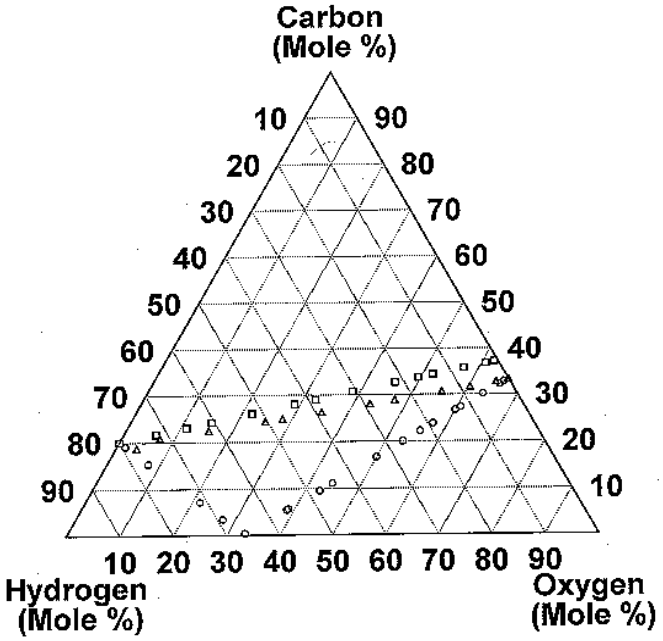

Figure 2. Ternary phase diagram for the solid phase(s) present for graphite/gases (**F**), Fe/Fe_3O_4/gases (**G**), Fe/Fe_3C/gases mixtures at equilibrium at 200°C and 15 atm. ([a]) (gases = H_2O, CO, CO_2, H_2 and CH_4).

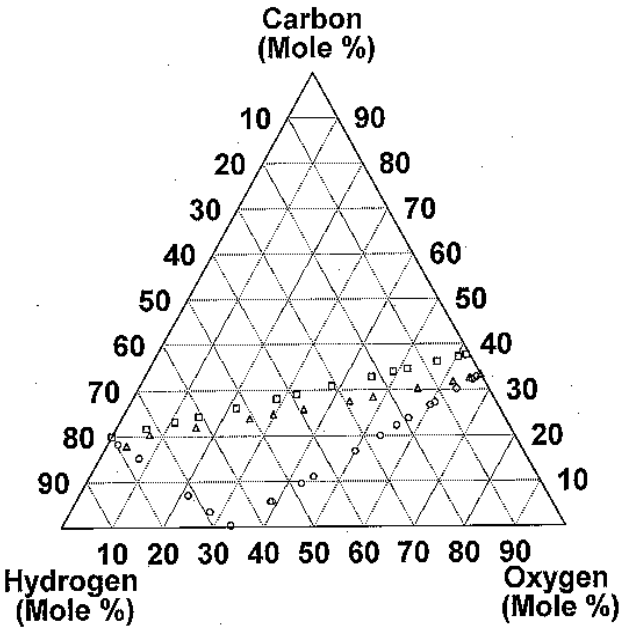

Figure 3. Ternary phase diagram for the solid phase(s) present for graphite/gases (**"**), Fe/Fe_3O_4/gases (**G**) and Fe/Fe_3C/gases mixtures at equilibrium at 250°C and 15 atm. (gases = H_2O, CO, CO_2, H_2 and CH_4).

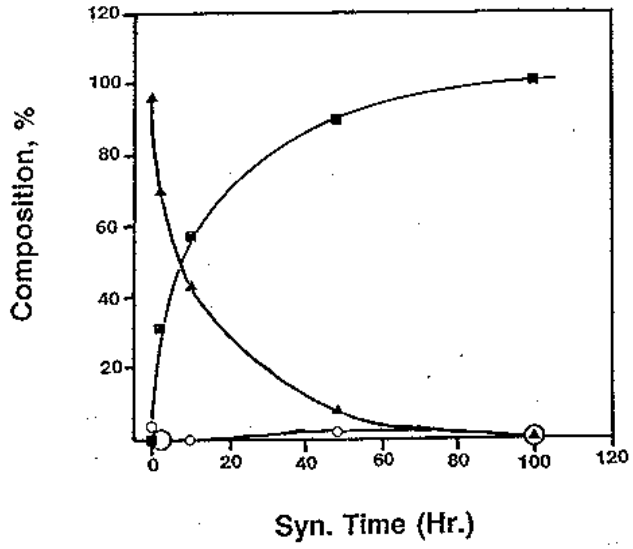

Figure 4. Change in composition of an activated iron catalyst during synthesis. Fe_3O_4 (**O**), Fe_2O_3 (**F**), and Fe carbides (>) (high surface, 300 m^2/g, 3.0 nm Fe_2O_3) (from ref. 5).

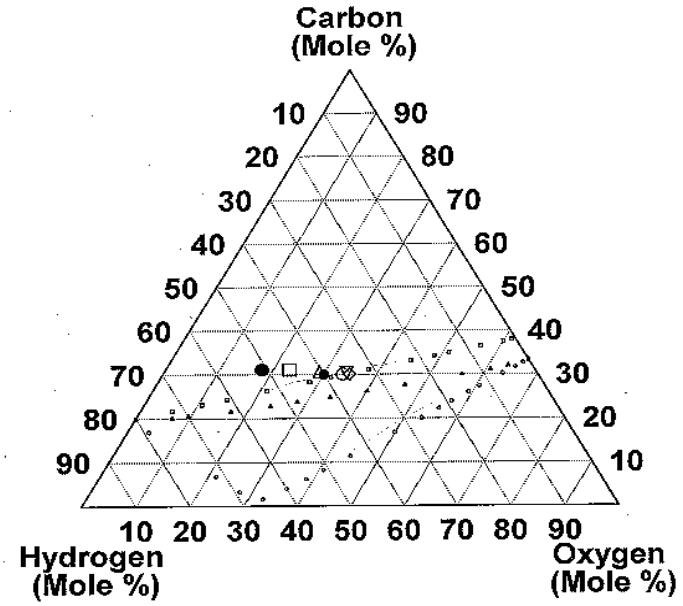

Figure 5. The gas phase composition during synthesis at various flow rates plotted on the ternary phase diagram of Figure 1. Data #1 in Table 1 (**!**), data #2 (**G**), data #3 (ª), data #4 (•), data #5 («), data #6 (**"**) and feed composition of $H_2/CO = 0.67$ (**!**).

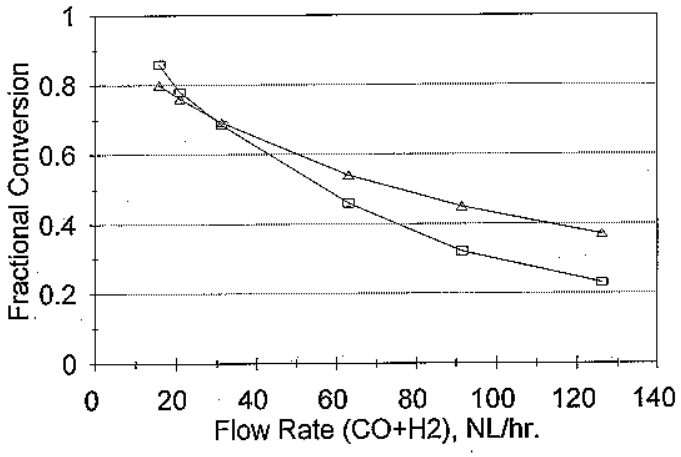

Figure 6. The variation of the conversion of H_2 and CO with flow rate ($H_2/CO = 0.7$, 270°C and 170 psig) (from ref. 9) (X, H_2 (ª) and X, CO (**G**).

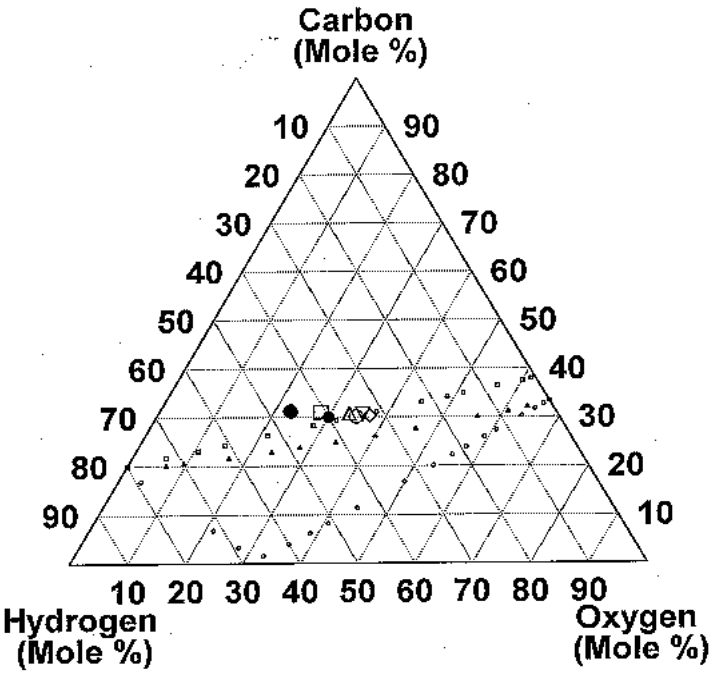

Figure 7. The gas phase composition during synthesis at various flow rates plotted on the ternary phase diagram of Figure 1 (both liquid and gaseous CO,H_2 and CO_2 and H_2O are included in the calculation). Data #1 in Table 1 (**!**), data #2 (**G**), data #3 (ª), data #4 (•), data #5 («), data #6 (**"**) and feed composition of $H_2/CO = 0.67$ (**!**).

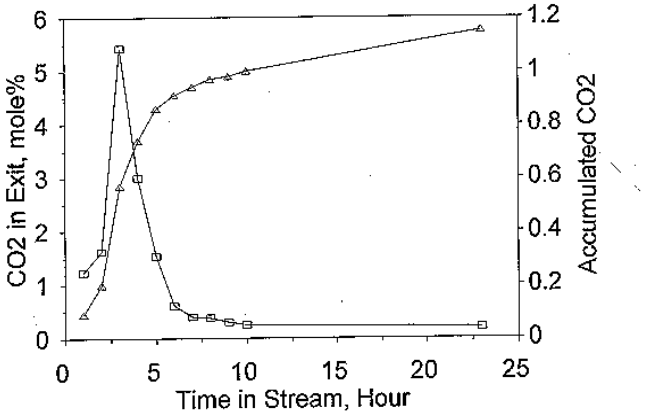

Figure 8. Rate of generation of CO_2 during activation of an iron catalyst at 270°C in a flow of CO in a 2 inch x 6 foot slurry bubble column reactor. CO_2 in exit (**G**) and accumulated CO_2 (Î).

3.1.4 Activation Study of Precipitated Iron Fischer-Tropsch Catalysts

ABSTRACT

Slurry phase Fischer-Tropsch Synthesis (FTS) was conducted with two precipitated iron catalysts (100Fe/3.6Si/0.71K and 100Fe/4.4Si/1.0K, atomic % relative to Fe) at 543K, 1.31MPa and a synthesis gas (H_2/CO=0.7) space velocity of 3.1 NL h^{-1} g Fe^{-1}. The impact of activation gas (CO, H_2/CO=0.7 or H_2/CO=0.1), temperature (543K or 573K) and pressure (1.31MPa or 0.10 MPa) on the long term (>500 h) activity and selectivity of the catalysts were explored. Pretreatment with CO under the conditions employed gave highly active and stable catalysts. Catalyst performance when synthesis gas activation was used was found to be dependent upon the partial pressure of hydrogen in the activating gas with low hydrogen partial pressures resulting in the highest catalyst activity. X-ray diffraction results indicate that carbon monoxide activations and synthesis gas activations with low hydrogen partial pressure result in the formation of the carbides ?-Fe_5C_2 and e-$Fe_{2.2}C$ while activation with synthesis gas with high hydrogen partial pressure results in the formation of only Fe_3O_4. It was found that treating the 100/3.6Si/0.71K catalyst activated with synthesis gas at 1.31 MPa and 543K, with carbon monoxide caused the activity to increase dramatically and the Fe_3O_4 to be partially converted to iron carbides. It is concluded that Fe_3O_4 is relatively inactive for FTS while the presence of some bulk iron carbide is necessary for high FTS activity to be achieved.

INTRODUCTION

The activation procedure used for iron based Fischer-Tropsch synthesis (FTS) catalysts has a great influence on their activity and selectivity [1]. Reduction of fused

magnetite catalysts with hydrogen at high temperatures (>673K) and high linear flow rates is necessary to produce a substantial surface area necessary for good activity; however, reduction with synthesis gas or carbon monoxide is ineffective [2]. In contrast, activation of precipitated iron catalysts is not understood as well. Precipitated catalysts have been reported to be successfully activated with carbon monoxide [3,4] hydrogen [2,5] or synthesis gas [6-8].

Several research groups have reported that pretreatment of precipitated iron oxide with carbon monoxide is the preferred activation procedure. Bukur et al. have reported that pretreatment of doubly promoted Fe/Cu/K catalysts with carbon monoxide or synthesis gas (H_2:CO~0.7 or 2.0) results in higher initial activity and a heavier product than activation with hydrogen; however, hydrogen pretreatments were reported to result in more stable catalysts [4,5]. Pennline et al. found that activation of a precipitated iron-manganese catalyst with carbon monoxide was superior to activation with hydrogen or synthesis gas at 15 MPa and 548 K; furthermore, they report little temperature or pressure affects when activating with carbon monoxide [9]. During the initial German work on FTS, the Kaiser Wilhelm Institute favored pretreating catalysts with carbon monoxide at subatmospheric pressure [10]. In addition, Huang et al. have reported that an ultrafine iron oxide catalyst has superior activity when pretreated with carbon monoxide than with hydrogen or synthesis gas (H_2:CO=1.0) at 533 K and 0.79 MPa [11].

Although pretreatment of precipitated iron catalysts with carbon monoxide leads to active catalysts, hydrogen pretreatment is more favorable on an industrial scale, because it is less expensive and easier to purify. In general, pure hydrogen can be

prepared from synthesis gas using a membrane separation process that allows only hydrogen to pass; however, this separation will not lead to pure carbon monoxide, but instead will produce a carbon monoxide rich synthesis gas. SASOL utilizes hydrogen pretreatment of precipitated iron catalysts used in its commercial FT reactors [2]. In addition, much of the early German work utilized hydrogen pretreatment, i.e., Ruhrchemie AG, IG Farbenindustrie AG and Lurgi [10]. Hydrogen pretreatment has the disadvantage that the metallic iron that is formed is susceptible to sintering. High flow rates are needed to keep the partial pressure of water low and low temperatures are necessary to insure that a high surface area is maintained [2,5].

The development of a pretreatment procedure utilizing synthesis gas that would consistently lead to active catalysts would be attractive, because pretreatments could be performed with the same gas that is used in the FTS, thereby eliminating the need for a pure hydrogen or carbon monoxide stream. Kölbel and Ralek [6] and Mobil [7,8] have reported high activity and good stability with precipitated Fe/Cu/K catalysts in laboratory and demonstration plant slurry reactors using *in situ* synthesis gas activation. Pretreatment conditions appear to be crucial in determining the ultimate FT activity of synthesis gas activated catalysts. Kolbel and Ralek report that the temperature of the synthesis gas pretreatment is critical to the final activity and selectivity of the catalyst; too high a temperature will result in “supercarbonization” and too low a temperature will prevent activation [6]. In addition, pressure may also affect the ultimate activity; many of the German companies preferred activation at a low pressure when using synthesis gas pretreatments [10].

The catalyst phase that exists is strongly dependent on the activation procedure employed. Activation with hydrogen, carbon monoxide or synthesis gas generally result in the rapid formation of Fe_3O_4 [3]. With additional time, the Fe_3O_4 is converted to metallic iron in the case of hydrogen pretreatment or various iron carbides (usually ?-Fe_5C_2 or e-$Fe_{2.2}C$) with carbon monoxide or synthesis gas pretreatment [1-3,5]. During synthesis, metallic iron is rapidly converted to iron carbide and with longer times on stream the iron carbide may be oxidized to Fe_3O_4 [1-3,5]. Several studies have been made to correlate catalyst composition with activity [3,12-15]. Some reports claim iron carbides are active for FTS [12] while others claim an oxide species is responsible for activity [16]. In contrast, it has also been reported that a correlation between catalyst activity and bulk phase composition cannot be made [1-3].

The present study is aimed at providing a better understanding of the relationship between pretreatment, FTS activity and the phase composition of precipitated iron catalysts used in a slurry reactor. A comparison is made between pretreatment with carbon monoxide and synthesis gas (H_2:CO=0.7 or 0.1) with particular attention being paid to the affect of temperature and pressure used during the activation procedure on the resulting FTS activity.

EXPERIMENTAL

Catalysts were prepared by continuous precipitation of amorphous ferric oxyhydroxide from aqueous iron(III) nitrate nonahydrate (1.17M) and concentrated ammonium hydroxide (15.6M) in a continuous stirred tank reactor at pH 9.5. Hydrolyzed tetraethyl orthosilicate was added to the iron(III) nitrate solution to give the desired level of silicon. The catalyst slurry was filtered continuously with one or more

six inch rotary drum vacuum filters. The resulting catalyst cake was washed and filtered twice with a volume of distilled deionized water equal to the volume of the previous filtrate. A 5 kg catalyst batch was precipitated in this manner, oven dried in flowing air at 393 K and crushed to -300 mesh. The composition of this catalyst in terms of atomic percent relative to Fe is 100Fe/3.6Si. During loading into the slurry reactor, the catalyst was treated with sufficient potassium *t*-butoxide to make the composition 100Fe/3.6Si/0.71K. A large 75 kg catalyst batch was also prepared; however, this catalyst was prepared by adding potassium nitrate to the slurry, spray dried and calcined in air at 623 K. The composition of this catalyst was 100Fe/4.4Si/1.0K.

All FTS runs were conducted in a one liter autoclave operating as a continuous stirred tank reactor (CSTR). Catalysts were suspended in Ethylflo 164 hydrocarbon oil (Ethyl Corporation) which is reported to be a C_{30} 1-decene homopolymer. All catalysts loadings were 10 weight per cent unless otherwise noted. A schematic of the reactor system is shown in Figure 1. Hydrogen and carbon monoxide feed gas flow rates were controlled by two mass flow controllers (Brooks Instruments) with the resulting synthesis gas composition regulated by adjusting the flow rate of the appropriate gas. The synthesis gas, after passing through a 2 L mixing vessel, was delivered to the catalyst slurry through a dip tube that extended to below the impeller blade. The reactor effluent exited the reactor and passed sequentially through two traps maintained at 333 K and 273 K. Accumulated reactor wax was removed daily through a tube fitted with a porous metal filter (0.5 μm). Uncondensed effluent was sent to an on-line Carle gas analyzer for determination of carbon monoxide, hydrogen, carbon

dioxide, methane and C_2-C_4 alkanes and alkenes. An on-line Hewlett-Packard 5790 GC equipped with a Porpack-Q column was utilized for C_4-C_9 quantification. Liquid samples were analyzed with a Hewlett-Packard 5890 GC equipped with a 60 m DB-5 capillary column. The reactor was also equipped with a tube that extended below the liquid level which permitted catalyst slurry samples to be withdrawn periodically.

Catalysts were pretreated with carbon monoxide or activated with synthesis gas with a hydrogen:carbon monoxide ratio of 0.7 or 0.1. In general, the activation gas flow was started at ambient conditions, the necessary reactor pressure was set and the reactor was ramped to the desired temperature at 2 K min^{-1}. After reaching the activation temperature, the conditions were maintained for 24 h. Following the activation treatment, the reactor was brought to reaction conditions: hydrogen:carbon monoxide ratio of 0.7, 3.1 NL $h^{-1}g^{-1}$(Fe) (NL corresponds to 273 K, 0.10 MPa) 543 K and 1.31 MPa.

Catalyst samples were Soxhlet extracted according to the method of McCartney et al., [17] to remove accumulated wax and then analyzed by X-ray diffraction. Powder X-ray diffraction patterns of the catalysts were obtained using a Philips APD X-ray diffraction spectrometer equipped with a Cu anode and Ni filter operated a 40Kv and 20Ma (CuKa=1.5418 D). Iron phases were identified by comparing diffraction patterns of the catalyst samples with those in the standard powder X-ray diffraction file compiled by the Joint Committee on Powder Diffraction Standards published by the International Center for Diffraction Data.

RESULTS AND DISCUSSION

Catalyst Activation

Early in our efforts to develop an effective activation procedure for precipitated iron catalysts, we found that a 24 h treatment with carbon monoxide at 543 K and 1.31 MPa consistently resulted in highly active and stable catalysts (Figures 2a and 3). Initial carbon monoxide conversion for the 100Fe/3.6Si/0.71K and 100Fe/4.4Si/1.0K catalysts activated in this manner were 92% and 85%, respectively, with corresponding deactivation rates of 4.8% and 1.0% per week, respectively. Hydrocarbon productivities typically were in the range of 160-170 g m^{-3} ($CO+H_2$ feed) with greater than 80% being C_3 and higher. The reproducibility of this activation procedure has facilitated screening large numbers of catalysts so that reliable data concerning optimum promoter levels can be determined. Much of this work is directed at developing a process for catalyst preparation that is suitable for scale-up to pilot plant scale.

The use of pure carbon monoxide as an activation gas is acceptable for small laboratory reactors; however, it is cost prohibitive for a pilot plant. As a result, it is economically attractive and operationally more facile to be able to activate catalysts *in situ* with the same synthesis gas as used during the FTS. Activity and selectivity results of our initial efforts using synthesis gas activation are shown in Table 1. Treatment of either 100Fe/3.6Si/0.71K or 100Fe/4.4Si/1.0K catalysts with synthesis gas (H_2:CO=0.7) at 3.1 NL $h^{-1}g^{-1}$(Fe), 543 K and 1.31 MPa resulted in poor FTS activity. Carbon monoxide conversions were typically below 30% and did not increase appreciably with time on stream. Kölbel and Ralek have reported successful synthesis

gas activations with a precipitated Fe/Cu/K catalyst at 0.8-1.5 MPa and at a “formation” temperature 15-30 K above the FTS temperature (~573 K); however, they report that at too high a temperature carbon will form and at too low a temperature the formation will not take place and the catalyst will be inactive [6]. In contrast, we have found that increasing the activation temperature to 573 K while maintaining the pressure at 1.31 MPa has little affect on conversion during synthesis with catalysts activated with synthesis gas.

During the Reichsamt comparative experiments conducted in Germany in 1943, the Kaiser Wilhelm Institute, Brabag and Rheinpreussen all activated their iron catalysts with synthesis gas or water gas at atmospheric or subatmospheric pressure [10]. To explore the possible affect of pressure on synthesis gas activation, both 100Fe/3.6Si/0.71K (Figure 3) and 100Fe/4.4Si/1.0K (Figure 2c) catalysts were treated with synthesis gas (H_2:CO=0.7) at 3.1 NL $h^{-1}g^{-1}$(Fe), 0.10 MPa and 543 K for 24 h. A dramatic increase in activity was observed as compared to when the same activation was conducted at 1.31 MPa. For both the 100Fe/3.6Si/0.71K and 100Fe/4.4Si/1.0K catalysts, the initial carbon monoxide conversion was greater than 85% which is comparable to that obtained when pretreating with carbon monoxide at 543 K and 1.31 MPa. In fact, the 100Fe/4.4Si/1.0K catalyst had an initial conversion of 92% and displayed remarkable stability, deactivating at an average rate of only 0.59% per week for over 2700 h. In addition, the 100Fe/4.4Si/1.0K catalyst was also activated with synthesis gas (H_2:CO=0.7) at 573 K and 0.10 MPa. As was found when activating with synthesis gas at 1.31 MPa, increasing the temperature had little affect on the initial

carbon monoxide conversion (Figure 2d); however, the deactivation rate was higher at 1.6% per week.

It is interesting to note that no such pressure dependence was observed with carbon monoxide pretreatment (Figure 2b). Pretreating the 100Fe/4.4Si/1.0K catalyst with carbon monoxide for 24 h at 543 K and 1.31 MPa resulted in an initial conversion slightly lower than when activating at 0.10 MPa; however, after 72 h at synthesis conditions, the conversions were essentially the same in both cases.

Selectivity data at high conversion for the 100Fe/4.4Si/1.0K catalyst activated with carbon monoxide or synthesis gas are presented in Table 2. In general, carbon monoxide activations resulted in the production of less methane and more liquid products than activations with synthesis gas. At comparable conversions, the catalyst activated with carbon monoxide at either 543 K/1.31 MPa or 543 K/0.10 MPa produced up to twice as much C_{12}+ as when activated with synthesis gas at 0.10 MPa. In contrast, Bukur et al. reported similar selectivities for a doubly promoted Fe/Cu/K catalyst that was activated with carbon monoxide or with synthesis gas [5].

The fact that pretreatment with carbon monoxide at either 0.10 or 1.31 MPa results in similar FTS activity suggests that the pressure dependence of synthesis gas activation is due to the presence of hydrogen. To test this possibility, the 100Fe/3.6Si/0.71K catalyst was treated with a synthesis gas low in hydrogen (H_2:CO=0.1) for 24 h at 2.1 NL $h^{-1}g^{-1}$(Fe), 543 K and 1.31 MPa. The initial carbon monoxide conversion was approximately 65% which is intermediate between activation with pure carbon monoxide and synthesis gas with a hydrogen:carbon monoxide ratio of 0.7. As shown in Figure 4, there is a clear correlation between the partial pressure

of hydrogen in the activating gas and the carbon monoxide conversion obtained during the early synthesis period.

Catalyst Characterization

Catalyst slurry samples were removed from the reactor for the series of runs with the 100Fe/3.6Si/0.71K catalyst. X-ray diffraction analysis of the catalyst following pretreatment with CO (Figure 5a) or synthesis gas at 0.10 MPa (Figure 5b) shows the presence of Fe_3O_4 and the carbides ?-Fe_5C_2 and e-$Fe_{2.2}C$. In addition, X-ray diffraction data for the catalyst activated with hydrogen lean synthesis gas (H_2:CO=0.1) (Figure 5c) showed Fe_3O_4 and small amounts of iron carbides. In contrast, X-ray diffraction analysis of the catalyst activated with synthesis gas at 1.31 MPa showed only Fe_3O_4 (Figure 5d).

As discussed above, the carbon monoxide conversion of the 100Fe/3.6Si/0.71K catalyst activated with synthesis gas (H_2:CO=0.7) at 1.31 MPa and 543 K never rose above 12%. After 96 h of synthesis, the hydrogen flow was stopped and the catalyst was treated with carbon monoxide under the same operating conditions for 22 h. Following the carbon monoxide treatment, the hydrogen flow was resumed and the activity of the catalyst was found to rapidly increase (Figure 6). The ultimate activity of catalyst was similar to that obtained for the carbon monoxide pretreated catalyst. X-ray diffraction analysis shows that the catalyst consists of only Fe_3O_4 prior to the carbon monoxide treatment; however, following the carbon monoxide treatment, the catalyst consists of a mixture of Fe_3O_4, ?-Fe_5C_2 and e-$Fe_{2.2}C$ (Figure 7). These results are consistent with the Fe_3O_4 phase being relatively inactive for FTS while ?-Fe_5C_2 and e-$Fe_{2.2}C$ are necessary for high FTS activity. This does not necessarily imply that ?-

Fe_5C_2 and e\-$Fe_{2.2}C$ are active phases for FTS, in fact, previous works have shown that there is no correlation between the amount of bulk iron carbide present and the activity of the catalyst [2,3]. It is possible; however, that the presence of a bulk iron carbide is necessary to serve as a support for an active surface species. In considering the above results and discussion, it should be kept in mind that the characterization is based upon XRD; therefore, only bulk phases are detected.

The overall Fischer-Tropsch Synthesis with iron catalysts can be approximated as the sum of the hydrogenation of carbon monoxide to methylene groups and the water-gas shift reaction.

$$x\mathrm{CO} + 2x\mathrm{H_2} \rightarrow x(\mathrm{-CH_2-}) + x\mathrm{H_2O} \quad (1)$$

$$y\mathrm{H_2O} + y\mathrm{CO} \rightarrow y\mathrm{CO_2} + y\mathrm{H_2} \quad (2)$$

$$(x+y)\mathrm{CO} + (2x-y)\mathrm{H_2} \rightarrow x(\mathrm{-CH_2-}) + (x-y)\mathrm{H_2O} + y\mathrm{CO_2} \quad (3)$$

For iron based catalysts, whether the catalyst exists as a carbide or as an oxide depends on the reducing behavior of the atmosphere present in the reactor. During Fischer-Tropsch synthesis, the catalyst is exposed to an atmosphere of hydrogen, carbon monoxide and the reaction products: water and carbon dioxide. It is well known that water and carbon dioxide will oxidize metallic iron and iron carbides to Fe_3O_4 [1,2]. Thermodynamic data on the metallic iron/iron oxide system show that at a H_2O:H_2 ratio > 0.03 or a CO_2:CO ratio > 2.8 oxidizing conditions exist and Fe_3O_4 is the stable phase compared to metallic iron [18]. Equation 3 can be used to calculate the H_2O:H_2 and CO_2:CO ratios based on the carbon monoxide and hydrogen conversions. During activation of the 100Fe/3.6Si/0.71K catalyst with synthesis gas at 1.31 MPa, the H_2O:H_2 ratio was 0.16 and the CO_2:CO ratio was 0.022. The water level clearly was high

enough to make Fe_3O_4 the thermodynamically stable phase during the activation which would explain why no iron carbides could be detected by XRD. This conclusion requires that the formation of iron carbides results from an iron species that is lower-valent than is present in Fe_3O_4. In contrast, synthesis gas activation of the same catalyst at 0.10 MPa had a much lower H_2O:H_2 ratio of 0.0070 and a CO_2:CO ratio of 0.90. These water and carbon dioxide levels were low enough to enable the catalyst to be reduced to form active iron carbides. It appears that by decreasing the hydrogen partial pressure, reaction 1 is suppressed enough during the activation that active iron carbides can be formed. An alternate method of activation with synthesis gas would be to operate at high linear flow rates (low conversion) to suppress water formation and to rapidly remove it from the reactor as is usually done when activating with pure hydrogen [2,5].

CONCLUSIONS

CO pretreatment of precipitated Fe/Si/K catalysts consistently results in high FTS activity because active carbide phases are readily formed. In the case of syngas activation, there is a relationship between the hydrogen partial pressure in the activation gas and the initial FTS activity. During activation with syngas, the catalyst is exposed to carbon dioxide and water as well as carbon monoxide and hydrogen. It has been found that during activations with high partial pressures of hydrogen, enough water is formed to prevent the catalyst from being reduced to active iron carbide phases and only relatively inactive Fe_3O_4 is formed. The results of this study indicate that the formation of an iron carbide (?-Fe_5C_2 and/or e-$Fe_{2.2}C$) is necessary for high FTS activity; however, based on previous Mössbauer spectroscopy experiments, the

activity of iron catalysts is not related to the amount of bulk iron carbide present [3]. These results indicate that a layer of surface carbide may be responsible for FTS activity.

ACKNOWLEDGMENT

This work was supported by the U. S. Department of Energy, contract no. DE-AC22-94PC94055 and the Commonwealth of Kentucky.

REFERENCES

1. R. B. Anderson, *The Fischer-Tropsch Synthesis*; Academic Press: Orlando, FL, 1984.
2. M. E. Dry, in Catalysis - Science and Technology; Anderson, J. R., Boudart, M., Eds; Springer-Verlag: New York, 1981; Vol. 1, pp. 159-255.
3. R. J. O'Brien, L. Xu, D. R. Milburn, Y.-X. Li, K. J. Klabunde and B. H. Davis, *Topics in Catalysis*, **2** (1995) 1.
4. D. B. Bukur, X. Lang, J. A. Rossin, W. H. Zimmerman, M. P. Rosynek, E. B. Yeh and C. Li, *Ind. Eng. Chem. Res.*, **28** (1989) 1130.
5. D. B. Bukur, M. Koranne, X. Lang, K. R. P. M. Rao and G. P. Huffman, *Appl. Catal.*, **126** (1995) 85.
6. H. Kölbel and M. Ralek, *Catal. Rev.-Sci. Eng.*, **21** (1980) 225.
7. J. C. W. Kuo, *Slurry Fischer-Tropsch/Mobil Two-Stage Process of Converting Syngas to High Octane Gasoline*, DOE/PC/30022-10, Final Report, June 1983.
8. J. C. W. Kuo, *Two Stage Process for Conversion of Synthesis Gas to High Quality Transportation Fuels*, DOE/PC/60019-9, Final Report, October 1985.
9. H. W. Pennline, M. F. Zarochak, J. M. Stencel and J. R. Diehl, *Ind. Eng. Chem. Res.*, **26**, (1987) 595.
10. Report on the Petroleum and Synthetic Oil Industry of Germany, Ministry of Fuel and Power, His Majesty's Stationary Office, London, 1946, pp. 96-100.
11. C.-S. Huang, L. Xu and B. H. Davis, *Fuel Sci. Technol. Int.*, **11** (1993) 639.
12. J. A. Amelse, J. B. Butt and L. H. Schwartz, *J. Phys. Chem.*, **82** (1978) 558.

13. J. W. Niemantsverdriet, A. M. van der Kraan, W. L. van Dijk, and H. S. van der Baan, *J. Phys. Chem.*, **84** (1980) 3363.

14. J. B. Butt, *Catal. Lett.*, **7** (1990) 61.

15. J. B. Butt, *Catal. Lett.*, **7** (1990) 83.

16. J. P. Reymond, P. Mériaudeau and S. J. Teichner, *J. Catal.*, **75**, (1982) 39.

17. J. T. McCartney, L. J. E. Hofer, B. Seligman, J. A. Lecky, W. C. Peebles and R. B. Anderson, *J. Phys. Chem.*, **57** (1953) 730.

18. T. B. Reed, *Free Energy of Formation of Binary Compounds: An Atlas of Charts for High -Temperature Chemical Calculations*; The MIT Press: Cambridge, MA, 1971.